



2015

14th Oxford Summer School on Neutron Scattering

Exercise Book

Useful Physical Constants	1
A) Coherent and Incoherent Scattering	2
B) Time-of-flight Powder Diffraction	5
C) Single Crystal Diffraction	10
D) Incoherent Inelastic Scattering	13
E) Coherent Inelastic Scattering	16
F) High Resolution Spectroscopy	22
G) Small Angle Scattering	26
H) Reflectometry	30
I) Polarized Neutrons	33
J) Spin-Echo Small Angle Neutron Scattering	35
K) Magnetic Scattering	39
L) Chemical Applications	41
M) Biological Applications	44
N) Disordered Materials Diffraction	48

The school is supported by:



Science & Technology Facilities Council

ISIS



<http://www.oxfordneutronschool.org>

6th – 18th September 2015

Values of Physical Constants

Constant	Symbol	SI Units	“Neutron” Units
Speed of light	c	$3.00 \times 10^8 \text{ m s}^{-1}$	
Electron charge	e	$1.60 \times 10^{-19} \text{ C}$	
Boltzmann's constant	k_B	$1.38 \times 10^{-23} \text{ J K}^{-1}$	0.086 meV K^{-1}
Planck's constant	h	$6.63 \times 10^{-34} \text{ J s}$	$4.14 \times 10^{-12} \text{ meV s}$
	$\hbar = h/2\pi$	$1.06 \times 10^{-34} \text{ J s}$	$6.59 \times 10^{-13} \text{ meV s}$
Avogadro's number	N_A	$6.02 \times 10^{23} \text{ mol}^{-1}$	
Mass of electron	m_e	$9.11 \times 10^{-31} \text{ kg}$	
Mass of proton	m_p	$1.67 \times 10^{-27} \text{ kg}$	
Bohr magneton	$\mu_B = e\hbar/2m_e$	$9.27 \times 10^{-24} \text{ J/T}$	
Nuclear magneton	$\mu_N = e\hbar/2m_p$	$5.05 \times 10^{-27} \text{ J/T}$	

Properties of the neutron

Mass, m_n	$1.67 \times 10^{-27} \text{ kg}$
Charge	0
Spin	1/2
Magnetic moment, μ_n	$-1.913 \mu_N$
Gyromagnetic ratio, γ_n	$1.832 \times 10^8 \text{ rad s}^{-1} \text{ T}^{-1}$

Relations between Units

$$1 \text{ meV} = 1.6 \times 10^{-22} \text{ J} = 0.24 \text{ THz} = 8.04 \text{ cm}^{-1} = 11.6 \text{ K}$$

A. Coherent and Incoherent Scattering

These exercises illustrate how to calculate coherent scattering amplitudes and incoherent scattering cross sections for nuclear scattering

Formulae

A neutron of spin $\frac{1}{2}$ interacts with a nucleus of spin I to form two states in which the spins are either parallel or antiparallel. The combined spin J of these states is $J = I + \frac{1}{2}$ and $J = I - \frac{1}{2}$, respectively. Different scattering lengths (amplitudes) b^+ , b^- are associated with these states. The probabilities (statistical weights) w^+ , w^- of the states are proportional to the number of spin orientations of each state. This number is $2J + 1$, so $w^+ \propto 2I + 2$ and $w^- \propto 2I$. By constraining $w^+ + w^- = 1$, we find

$$w^+ = \frac{I+1}{2I+1} \quad \text{and} \quad w^- = \frac{I}{2I+1} \quad (\text{A1})$$

Suppose that an atom has several isotopes and that the spin of the r^{th} isotope is I_r . The **coherent scattering length** b_{coh} of the atom is the scattering length averaged over all the isotopes and spin states, i.e.

$$b_{\text{coh}} = \bar{b} = \sum_r c_r (w_r^+ b_r^+ + w_r^- b_r^-) \quad (\text{A2})$$

where c_r is the abundance of isotope r , and w_r^+ and w_r^- are given by (A1) with I replaced by I_r .

We define the single-atom **coherent scattering cross section** by

$$\sigma_{\text{coh}} = 4\pi b_{\text{coh}}^2 = 4\pi \bar{b}^2 \quad (\text{A3})$$

The single-atom **total scattering cross section** is obtained by averaging the separate cross sections for each of the individual isotopes r in both possible spin states:

$$\begin{aligned} \sigma_{\text{tot}} &= 4\pi \sum_r c_r \{w_r^+ (b_r^+)^2 + w_r^- (b_r^-)^2\} \\ &= 4\pi \overline{b^2} \end{aligned} \quad (\text{A4})$$

Finally, the single-atom **incoherent scattering cross section** is the difference between the total and coherent cross sections:

$$\begin{aligned} \sigma_{\text{inc}} &= \sigma_{\text{tot}} - \sigma_{\text{coh}} \\ &= 4\pi (\overline{b^2} - \bar{b}^2) \end{aligned} \quad (\text{A5})$$

Exercises

A1 Table A.1 gives the nuclear spin I of the two most abundant isotopes of hydrogen, ^1H (protium) and ^2H (deuterium), together with the measured scattering lengths of the (neutron + nucleus) systems with combined spins $I + \frac{1}{2}$ and $I - \frac{1}{2}$. Calculate σ_{coh} and σ_{inc} for ^1H and ^2H .

Table A1

	spin I	b^+ (fm)	b^- (fm)
^1H (protium)	$\frac{1}{2}$	10.82	-47.4
^2H (deuterium)	1	9.53	0.98

$$1 \text{ fm} = 10^{-15} \text{ m}$$

You should find that σ_{coh} for ^1H and ^2H are quite different. This means that the scattering from certain parts of a hydrogen-containing sample can be enhanced through selective replacement of the hydrogen atoms by deuterium, a process known as *isotopic labelling*.

You should also find that σ_{inc} for ^1H is much larger than that of ^2H , so that σ_{inc} for natural hydrogen is close to that of ^1H (natural hydrogen is 99.99% ^1H). Hence, neutron scatterers often try to minimise the amount of hydrogen-containing materials (like glue) in the neutron beam during their experiments. If hydrogen is present in the sample itself, then the background can be considerably reduced if the sample is prepared with deuterium instead of hydrogen.

A2 Table A.2 gives the experimental values of the scattering lengths and the abundance of the individual isotopes of nickel: ^{58}Ni , ^{60}Ni , ^{61}Ni , ^{62}Ni and ^{64}Ni . With the exception of ^{61}Ni , the isotopes have zero spin. Calculate the values of σ_{coh} and σ_{inc} for a natural nickel sample containing all five isotopes.

Table A2

Abundances, nuclear spins and scattering lengths of the isotopes of nickel

Isotope, r	abundance c_r	spin I_r	b_r^+ (fm)	b_r^- (fm)
58	68.3%	0	14.4	-
60	26.1%	0	2.8	-
61	1.1%	3/2	4.6	12.6
62	3.6%	0	-8.7	-
64	0.9%	0	-0.4	-

B. Time-of-Flight Powder Diffraction

B1.

(a) In a time-of-flight powder diffraction experiment the incident beam is pulsed, and with each pulse a polychromatic burst of neutrons strikes the sample. The different wavelengths, λ , in a pulse are separated by measuring their time-of-flight (t.o.f.), t , from source to detector. Using the table of physical constants at the back, show that the relation between wavelength and t.o.f. is given by

$$t (\mu\text{secs}) = 251.9 \times \lambda (\text{\AA}) \times L (\text{m})$$

where L is the total flight path between the source and detector.

(b) A powder diffractometer, with total flight path $L = 100$ m and scattering angle $2\theta = 170^\circ$, was used to obtain the powder diffraction pattern of perovskite, CaTiO_3 . Calculate the values of t for the three Bragg reflections with the longest times of flight. (CaTiO_3 crystallises in a primitive cubic lattice with a unit cell of edge $a_0 = 3.84$ \AA.)

(c) For a sample with a cubic unit cell, show that the time-of-flight t of each Bragg peak in the t.o.f. powder diffraction pattern is related to its indices H, K, L by:

$$t \propto (H^2 + K^2 + L^2)^{-1/2} \quad (\text{B1})$$

B2.

Silicon crystallises in the face-centred-cubic (fcc) structure of diamond with the lattice points at:

$$0, 0, 0; \quad \frac{1}{2}, \frac{1}{2}, 0; \quad \frac{1}{2}, 0, \frac{1}{2}; \quad 0, \frac{1}{2}, \frac{1}{2}$$

In this structure there is a primitive basis of two identical atoms at $0,0,0$ and $\frac{1}{4}, \frac{1}{4}, \frac{1}{4}$ which is associated with each lattice point of the unit cell.

(a) Show that the Miller indices H, K, L of the Bragg reflections for the fcc lattice are all odd or all even.

(b) Show that reflections with an integer and odd value of $(H + K + L)/2$ such as (222) and (442) , are forbidden in this structure.

(c) From eqn. (B1) the Bragg reflections in the powder diffraction pattern are separated according to their values of $(H^2 + K^2 + L^2)$. In table B.1 all the possible values of $(H^2 + K^2 + L^2)$ are listed in the order of decreasing time-of-flight in the range;

$$3 \leq (H^2 + K^2 + L^2) \leq 40$$

(This is the range covered in Figure B1)

Table B1.

Sums of three squared integers.

$H^2+K^2+L^2$	$H^2+K^2+L^2$	$H^2+K^2+L^2$	$H^2+K^2+L^2$
3*	12*	21	32*
4*	13	22	33
5	14	24*	34
6	16*	25	35*
8*	17	26	36*
9	18	27*	37
10	19*	29	38
11*	20*	30	40*

The values of $(H^2+K^2+L^2)$ in which the integers are all odd or all even are marked with asterisks.

- (i) What are the indices H, K, L , corresponding to these asterisks?
- (ii) Which of the fcc reflections are forbidden?
- (iii) Which of the allowed fcc reflections overlap with one another?

(d) Figure B1 shows the diffraction pattern of powdered silicon, taken with the time-of-flight diffractometer HRPD at the ISIS pulsed neutron source. The scattering angle was $2\theta = 90.8^\circ$ and the path length $L = 96.8$ m.

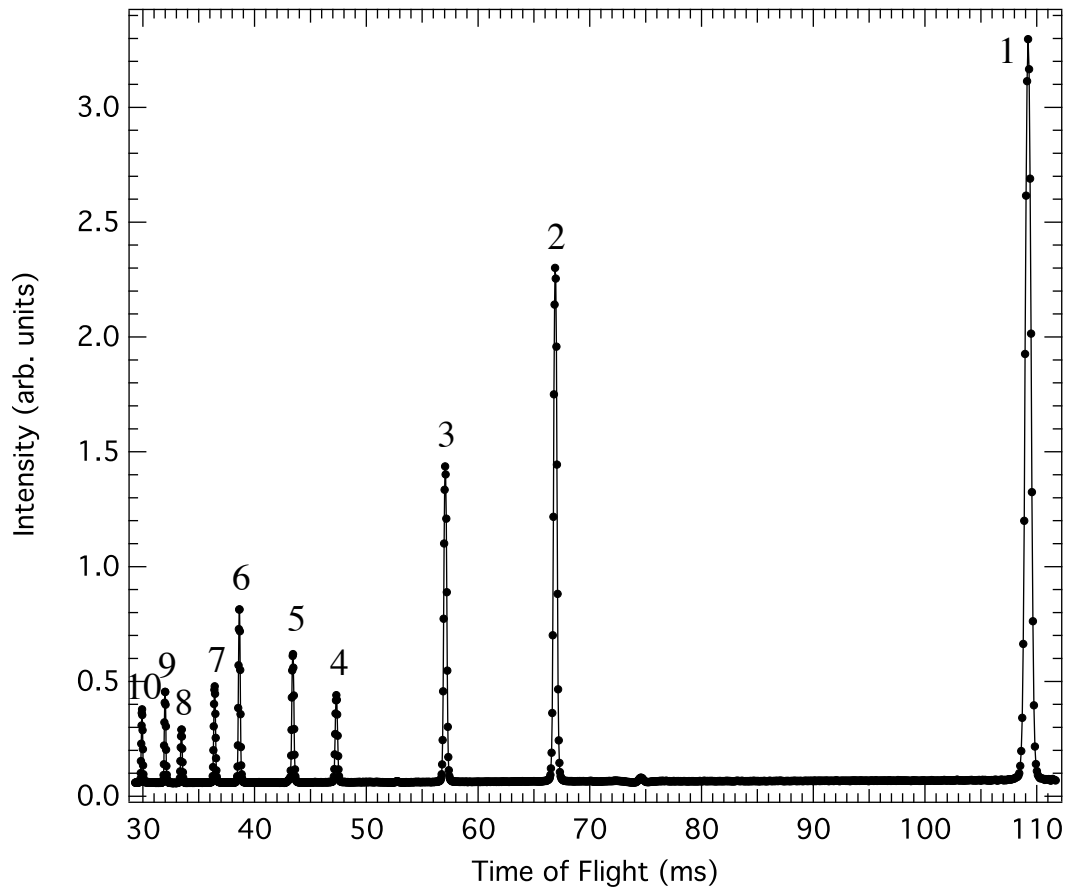


Figure B1. *Time-of-flight diffraction pattern of powdered silicon. The observed spectrum has been normalised to a vanadium spectrum: vanadium is an incoherent scatterer whose spectrum gives the wavelength dependence of the incident neutron flux.*

The values of t for the 10 numbered Bragg peaks in Figure B1 were measured (to a precision of better than 1 part in 10^5) giving the results in Table B2.

Index all these peaks and determine the linear size a_0 of the unit cell of silicon.

The position of the first peak appears to be shifted to lower time-of-flight than expected. Any ideas why?

Table B2

peak number	time of flight (ms)
1	109.232
2	66.912
3	57.066
4	47.320
5	43.424
6	38.636
7	36.426
8	33.457
9	31.991
10	29.923

B3.

In a t.o.f. neutron powder diffractometer, a sharp pulse of neutrons with a range of wavelengths is fired at the sample. The diffracted signal is measured at a fixed scattering angles 2θ , and the diffraction patterns comes about from measurements of the time taken for the neutrons in a single pulse to travel the distance L from the source to the detector. Using the de Broglie relationship together with the Bragg's Law, show that the time t taken by the neutrons to travel the distance L is related to the d -spacing of a given Bragg reflection by

$$d = \frac{ht}{2mL \sin \theta} \quad (\text{B2})$$

where m is the mass of the neutron.

For an uncertainty of $\Delta\theta$ in the scattering angle (caused by beam divergence, or finite sample/detector width), error analysis gives the corresponding uncertainty in the d -spacing:

$$\Delta d = \frac{\partial d}{\partial \theta} \Delta \theta \quad (\text{B3})$$

Show by differentiation of Bragg's law that for a given uncertainty $\Delta\theta$ this leads to a maximum resolution in the d -spacing of

$$\left| \frac{\Delta d}{d} \right| = \cot \theta \Delta \theta \quad (\text{B4})$$

In order to maximize the resolution of a t.o.f. powder diffractometer, the scattering angle 2θ is chosen to be as close to 180° as possible (backscattering detector banks). In this case a significant source of uncertainty is in the distance travelled by the neutron beam. Show that the uncertainty in the flight path L of ΔL leads to a resolution limit of

$$\frac{\Delta d}{d} = \frac{\Delta L}{L} \quad (\text{B5})$$

If the only uncertainty in the value of L comes from the depth of a neutron moderator, 2 cm thick, calculate the flight paths necessary to achieve;

- (a) a moderate resolution of $\Delta d/d = 2 \times 10^{-3}$
- (b) a high resolution $\Delta d/d = 5 \times 10^{-4}$

Comment on your answers, and check out the real situation at the ISIS spallation neutron source by looking at the instruments POLARIS and HRPD from <http://www.isis.stfc.ac.uk>.

C. Single-Crystal Diffraction

C1.

2.20 km/sec is conventionally taken as a standard velocity for thermal neutrons. (For example, absorption cross sections are tabulated for this value of the velocity.)

(i) Using the de Broglie relation show that the wavelength of neutrons with this standard velocity is approximately 1.8 Å.

(ii) What is the kinetic energy of these neutrons? (See values of physical constants, p1)

(iii) What is the energy of an X-ray photon of wavelength $\lambda = 1.8 \text{ \AA}$?

(iv) Calculate the velocity of a neutron having the same energy as this X-ray photon.

C2.

A beam of “white” neutrons emerges from a collimator with a divergence of $\pm 0.2^\circ$. It is then Bragg reflected by the (111) planes of a monochromator consisting of a single-crystal of lead.

(i) Calculate the angle between the direct beam and the [111] axis of the crystal to produce a beam of wavelength $\lambda = 1.8 \text{ \AA}$. (Unit cell edge a_0 of cubic lead is 4.94 Å)

(ii) What is the spread in wavelengths of the reflected beam?

Questions C3 and C4 are concerned with the treatment of Bragg scattering in reciprocal space. C3 refers to the scattering of neutrons of a fixed-wavelength, and C4 to the scattering of pulsed neutrons covering a wide band of wavelengths.

C3.

A single crystal has an orthorhombic unit cell with dimensions $a = 6 \text{ \AA}$, $b = 8 \text{ \AA}$ and $c = 10 \text{ \AA}$. Plot the reciprocal lattice in the $\mathbf{a}^*\text{-}\mathbf{b}^*$ plane adopting a scale of $1 \text{ \AA}^{-1} = 20 \text{ mm}$.

A horizontal beam of neutrons of wavelength $\lambda = 1.8 \text{ \AA}$ strikes the crystal. The crystal is rotated about its vertical \mathbf{c} axis between the settings for the (630) and (360) Bragg reflections. Draw the Ewald circles for these two reflections. How many $(HK0)$ reflections will give rise to Bragg scattering while the crystal is rotated between (630) and (360) ?

C4.

A pulse of neutrons with a wavelength range from 1.8 \AA to 5.0 \AA undergoes Bragg scattering from this crystal. The neutron beam is parallel to the \mathbf{a} axis of the crystal and strikes the crystal at right angles to the \mathbf{c} axis. Using the Ewald construction find the maximum number of Bragg reflections which could be observed simultaneously in the horizontal scattering plane.

C5.

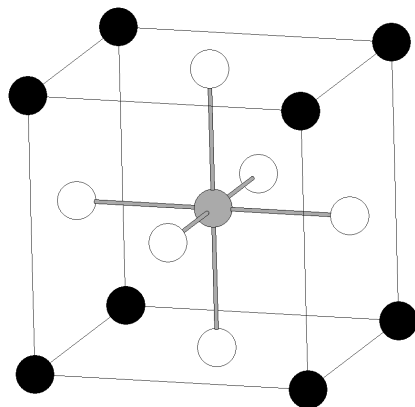


Figure C1

High-temperature cubic phase of BaTiO₃

Ba ²⁺	●	0, 0, 0
Ti ⁴⁺	●	1/2, 1/2, 1/2
O ²⁻	○	1/2, 1/2, 0; 1/2, 0, 1/2; 0, 1/2, 1/2

Coherent scattering lengths:

$$\begin{aligned}
 b_{\text{Ba}} &= 5.25 \times 10^{-15} \text{ m} \\
 b_{\text{Ti}} &= -3.30 \times 10^{-15} \text{ m} \\
 b_{\text{O}} &= 5.81 \times 10^{-15} \text{ m}
 \end{aligned}$$

atomic numbers:

$$\begin{aligned}
 Z_{\text{Ba}} &= 56 \\
 Z_{\text{Ti}} &= 22 \\
 Z_{\text{O}} &= 8
 \end{aligned}$$

(i) The diagram shows the high-temperature cubic unit cell of BaTiO₃ alongside a list of the fractional coordinates of the ions in the unit cell. Show that the intensity $I_{(00L)}$ of the neutron beam diffracted from the $(00L)$ planes of cubic BaTiO₃ is proportional to

$$[b_{\text{Ba}} + (-1)^L b_{\text{Ti}} + (1 + 2(-1)^L)b_{\text{O}}]^2,$$

where b_{Ba} , b_{Ti} and b_{O} are the coherent scattering lengths of the respective nuclei given above.

(ii) On cooling through the ferroelectric transition temperature $T_c = 130$ C the structure of BaTiO_3 undergoes a displacive transformation in which the Ti^{4+} and O^{2-} ions move in opposite directions relative to the Ba^{2+} ions. As a first approximation the fractional coordinates of the ions in the distorted phase are

$$\begin{array}{ll} \text{Ba}^{2+} & 0, 0, 0 \\ \text{Ti}^{4+} & \frac{1}{2}, \frac{1}{2}, \frac{1}{2} + \delta \\ \text{O}^{2-} & \frac{1}{2}, \frac{1}{2}, -\delta; \quad \frac{1}{2}, 0, \frac{1}{2} - \delta; \quad 0, \frac{1}{2}, \frac{1}{2} - \delta, \end{array}$$

where δ is a small displacement compared to the unit cell dimension.

The intensity of the (005) neutron diffraction peak from a single crystal of BaTiO_3 is found to increase by 74% on cooling the crystal through T_c . Use this observation to determine δ , under the assumption that it is small compared to the unit cell dimension.

(iii) Explain why it is advantageous to use neutron diffraction, rather than X-ray diffraction, to determine the ionic displacements. (Assume that the X-ray atomic scattering factors, f , for the (005) reflection are proportional to the atomic number Z .)

D. Incoherent Inelastic Scattering **(with a Pulsed Neutron Spectrometer)**

IRIS is an "inverted-geometry" spectrometer, which is installed at the ISIS pulsed neutron source in the UK. A white beam of neutrons coming from the moderator is first chopped to a smaller wavelength band and then guided to the sample. There are two choppers placed at 6.3m and 10m from the moderator. The scattered neutrons are then analysed using a pyrolytic-graphite crystal analyser. The 002 (or 004) planes of the analyser, Bragg reflect the neutrons to the detector. The distance from the moderator to the sample is 36.41m, and the distance sample-to-analyser-to-detector is 1.45 m. A schematic is shown below:

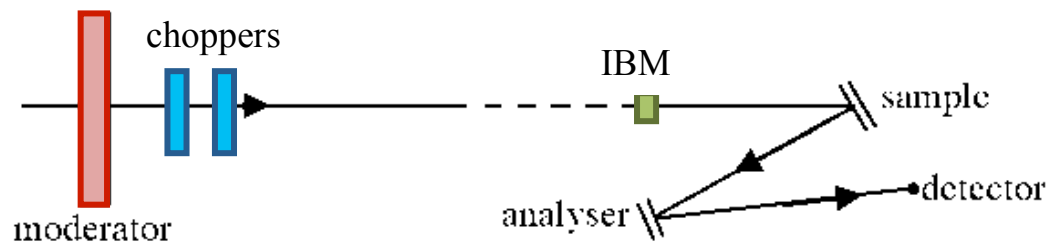


Figure D1. Schematic geometry of the IRIS spectrometer.

The spectrum shown in Figure D2 is for the IRIS incident monitor, which is placed at 0.355m before the sample (from the moderator direction). Note that ISIS runs at 50Hz with a time frame of 20ms.

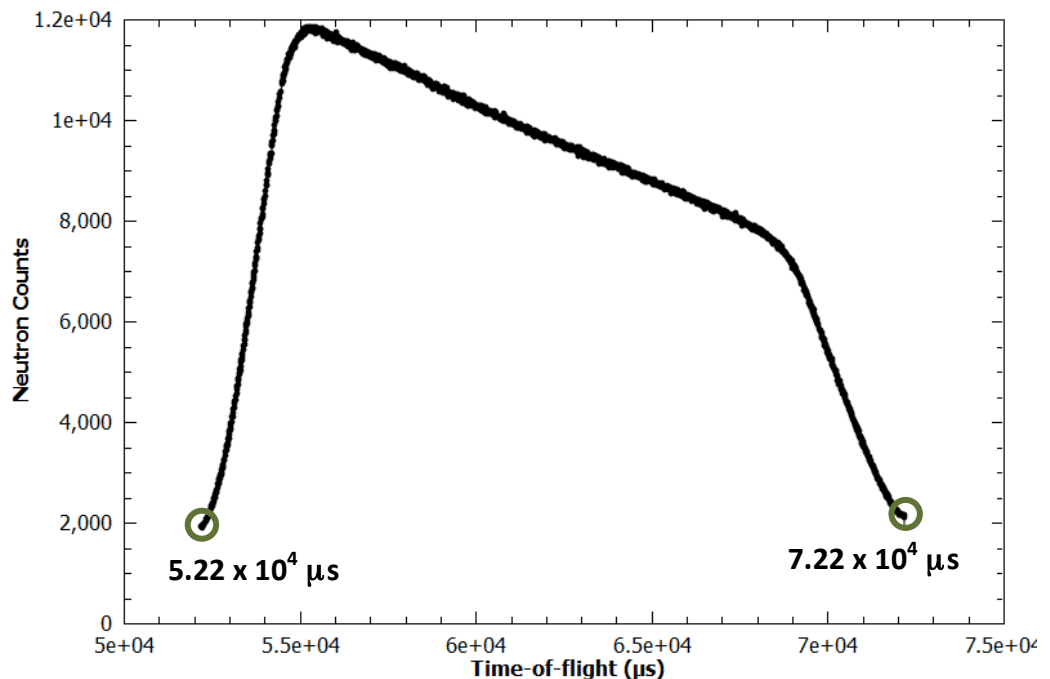


Figure D2. Incident monitor spectrum for PG002 configuration.

The IRIS spectrum shown in Figures D3 and D4 (zoomed in) is for a sample of an ionic liquid at 4K. The central peak corresponds to elastic scattering by the sample, and the two outer peaks arise from inelastic scattering due to the tunnelling of hydrogen atoms in methyl groups in the ionic liquid.

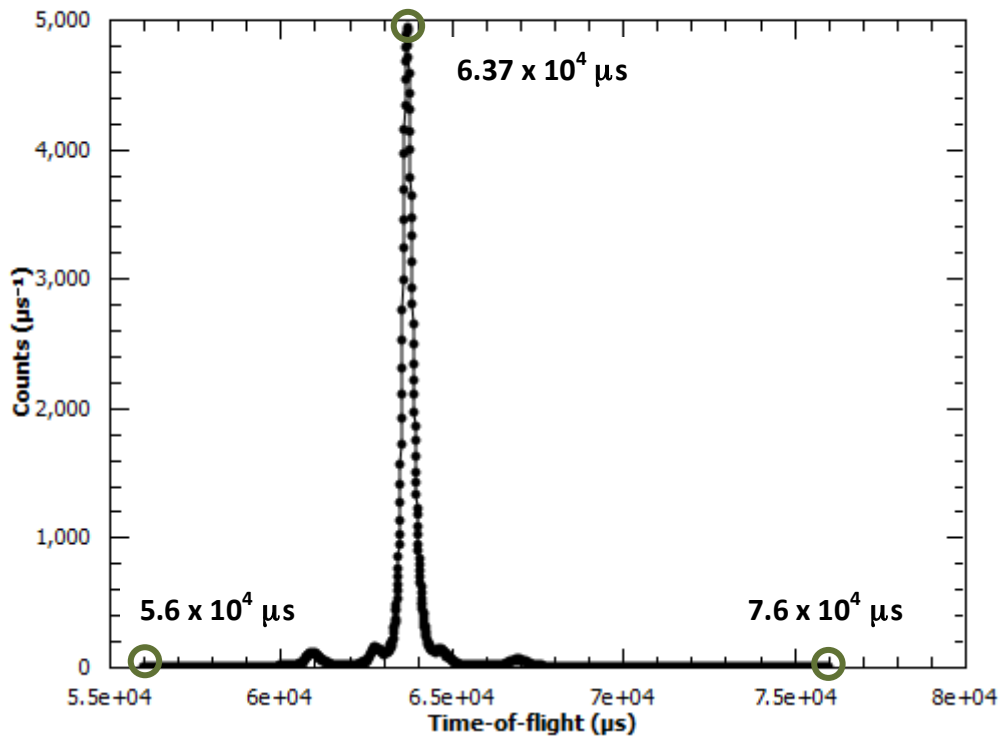


Figure D3. IRIS time-of-flight spectrum of an ionic compound at 4 K.

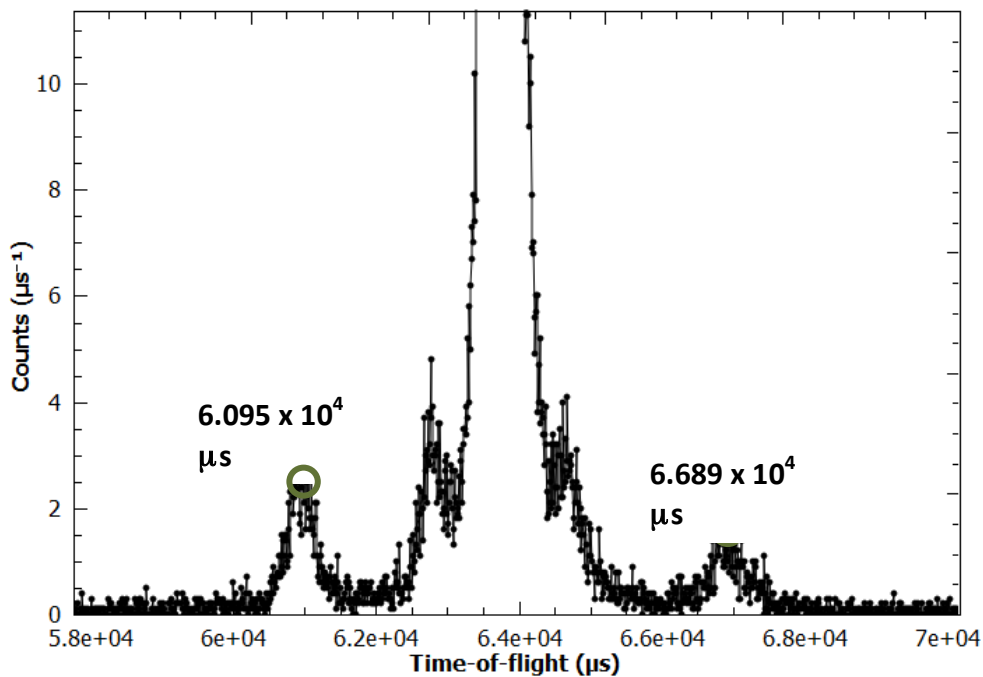


Figure D4. IRIS time-of-flight spectrum of an ionic compound at 4 K (zoomed in).

D1.

- (i) What is the energy selected by the crystal analyser for the data in Figure 3?
- (ii) The d -spacing of the (002) planes in pyrolytic graphite is 3.35 Å. What is the Bragg angle θ_A of the analyser?
- (iii) What is the advantage of using such a high take-off angle $2\theta_A$ for the analyser?

D2.

- (i) Looking at the monitor spectrum in figure D2, what is the incoming wavelength band?
- (ii) What is the magnitude of the energy transfer that can be measured with this wavelength band?
- (iii) Identify the inelastic peaks in the spectrum associated with neutron energy loss and neutron energy gain (Figures D3 and D4). Would this be the same in a direct geometry spectrometer?
- (iv) What is the magnitude of the energy transfer for the marked peaks?
- (v) Why are the intensities of the energy-gain and energy-loss peaks slightly different?

D3.

- (i) There are two choppers on the IRIS instrument, one at 6.3m and one at 10m. Why do we need two?
- (ii) The user wants to look at inelastic scattering features at higher energy transfers. Can it be done on IRIS? If so how? [Hint: do we need to change any settings? And if so are there any consequences?]
- (iii) How else could be change the energy window that we would look at?

E. Coherent Inelastic Scattering (with a Three-Axis Spectrometer)

One of the most important instruments used in neutron scattering is the three-axis spectrometer. A schematic drawing of the machine is shown in Figure E1. By employing a monochromatic neutron beam of a definite wave-vector \mathbf{k}_i (of magnitude $k_i = 2\pi / \lambda_i$ with λ_i the incident wavelength), which is incident on a single crystal in a known orientation, and by measuring the final wave-vector \mathbf{k}_f after scattering by the sample, we can examine coherent excitations such as phonons (in which the atoms are excited by thermal vibrations) or magnons (in which the spin system of the atom is excited).

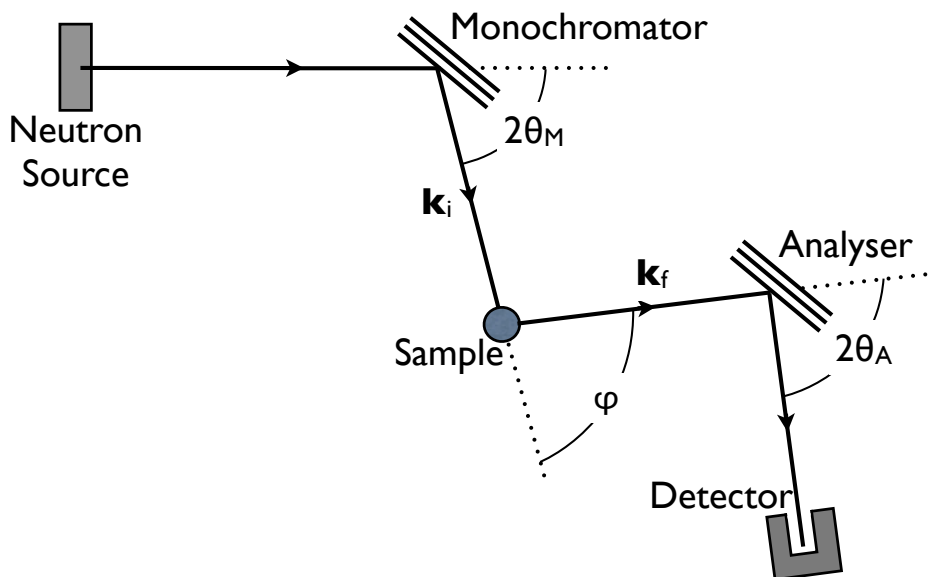


Figure E1. Three-axis spectrometer.

The three-axis instrument appears to be complicated, but it is conceptually simple and every movement may be mapped by considering the so-called scattering triangle (Figure E2). In practice, what is difficult about a three-axis machine is that there are many different ways of performing an experiment, and choosing the appropriate configuration is often the key to performing a successful experiment. This is in contrast to a powder diffraction experiment, where one simply puts the sample in the beam and records the diffraction pattern. (See Section B).

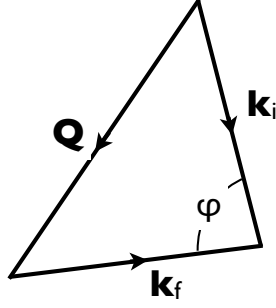


Figure E2. Scattering triangle representing the momentum $\hbar Q$ transferred to the sample when the wavevector of the neutron changes from k_i to k_f . ϕ is the scattering angle.

In the following we shall consider how one actually measures a phonon excitation, using various diagrams in reciprocal space to represent the process. We use formulae which apply to all scattering processes (both neutrons and X-rays).

Momentum conservation gives

$$\mathbf{Q} = \mathbf{k}_i - \mathbf{k}_f \quad (\text{E1})$$

where \mathbf{Q} is the scattering vector. If ϕ is the angle between k_i and k_f , we have

$$Q^2 = k_i^2 + k_f^2 - 2 k_i k_f \cos \phi \quad (\text{E2})$$

Energy conservation gives

$$\Delta E = E_i - E_f \quad (\text{E3})$$

where E_i is the energy of the incident neutron, E_f is its energy after scattering, and ΔE is the energy transferred to the scattering system. ΔE may be positive (neutrons lose energy) or negative (neutrons gain energy). If k is the wave-number of a neutron, its energy E is related to k by

$$E = 81.8 / \lambda^2 = 2.072 k^2 \quad (\text{E4})$$

where E is in meV, λ is in \AA and k is in \AA^{-1} .

For the following exercises, imagine that you wish to investigate the low-energy spectra of silver chloride, AgCl, which is a cubic crystal with a face-centred cubic unit cell. You have been allocated time on a three-axis spectrometer, which works with incident neutrons of energy from 3 to 14 meV.

Figure E3 shows the (HHL) plane of reciprocal space. The cubic lattice parameter a_0 of AgCl is 5.56 \AA . One reciprocal lattice unit (r.l.u.) is equal to $2\pi / a_0$ or 1.13 \AA^{-1} . The vector from the origin to any point HKL of the reciprocal lattice is of length, $2\pi / d_{\text{HKL}}$ where d_{HKL} is the spacing of the (HKL) planes in the real-space lattice.

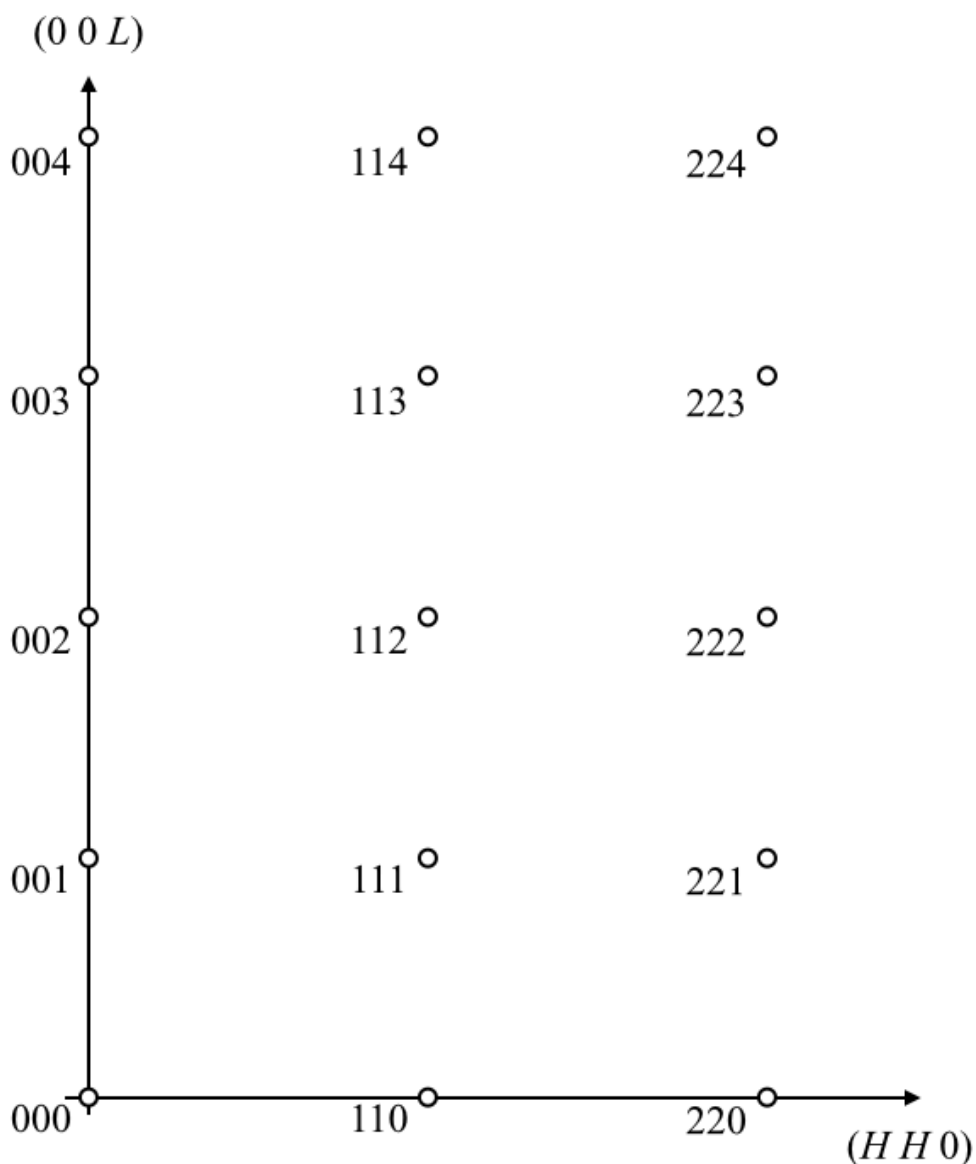


Figure E3. (HHL) plane in reciprocal space of cubic crystal.

E1

Which are the allowed points (giving non-zero Bragg reflections) of the reciprocal lattice in Figure E3? Mark them with a filled-in circle—they are the so-called zone-centres of the Brillouin zone. Leave the disallowed points as open points—these are the zone-boundaries of the Brillouin zone. (Note that the reciprocal lattice of a face-centred cubic crystal is a body-centred cubic lattice.)

E2

E_i ranges from 3 to 14 meV. Calculate the maximum and minimum values of the wavelength λ_i and the wave number k_i of the incident beam.

E3.

We shall begin our experiment using the maximum value of k_i and orienting our crystal to find the 220 Bragg reflection. The scattering we observe is elastic scattering, which is much stronger than the inelastic scattering.

(i) What is the magnitude of $Q_{220} = 2\pi / d_{220}$
Draw \mathbf{Q} , \mathbf{k}_i and \mathbf{k}_f for the 220 reflection.

(ii) What is the angle ϕ between \mathbf{k}_i and \mathbf{k}_f ?

(iii) What is the relation between the Bragg angle θ_B at the sample and ϕ ?

E4.

We can now start our inelastic experiment. Consider the dispersion curves for AgCl shown in Figure E4. Let us suppose that we wish to measure the phonon with a reduced wave vector of 0.4 propagating in the [00L] direction and that the phonon is transverse acoustic. (A shorthand notation for this is TA[00L].) Using the conversion constants on p1 we see that the energy of this phonon is about 3meV.

In Figure E3 draw the wave-vector \mathbf{q} of this phonon away from the 220 zone-centre. (By zone-centre we mean $q = 0$)

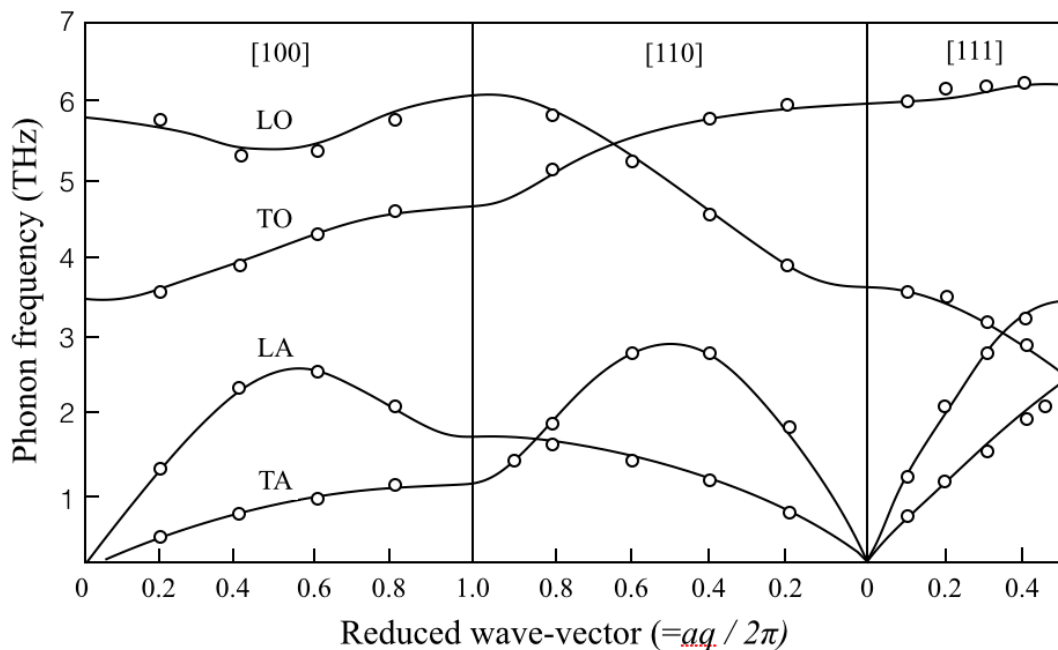


Figure E4. Phonon dispersion curves of cubic AgCl.

We will perform our experiment by using the maximum value of k_i .

E5.

Work out the possible values of k_f and ϕ . (There are two solutions depending on whether ΔE which is the phonon energy, is chosen to be positive or negative.)

E6.

It turns out that better resolution occurs for energy loss than for energy gain. Draw the configuration of k_i and k_f in Figure F3 for energy loss.

Another factor influencing the intensity which we observe in our experiment is the so-called Bose factor $n(E)$. This gives the population of phonon states at any given energy and temperature:

$$n(E) = \frac{1}{\exp(E/k_B T) - 1}$$

The intensity for neutron energy loss is proportional to $[1 + n(E)]$, whereas for neutron energy gain it is proportional to $n(E)$.

E7.

- (i) Calculate the Bose factors for the energy gain and energy loss

configurations in our example assuming that the sample is at a temperature of: (a) 300 K, (b) 0 K.

- (ii) Given the intensity relationships above, which way would we do the experiment with the sample at (a) room temperature, (b) liquid helium temperature?

E8.

Is it possible to measure the $TA[00L]$ phonon around the 440 reciprocal-lattice point ?

To map out the dispersion curves in Figure E4, we would do energy scans, say from 2 to 8 meV, at a series of q values between $[220]$ and $[221]$. A single peak would appear on each scan, giving the phonon energy for that reduced wave-vector.

E9.

Suppose an experiment is performed to measure the phonon dispersion curves of bcc potassium on a three-axis spectrometer, when the energy of the beam scattered into the analyser is held fixed at 3.5 THz. For a measurement of the LA mode at $\mathbf{Q} = [2.5, 0, 0]$, what will be the energy of the incident beam for an experiment in which the neutron beam loses energy in the creation of a phonon. The phonon dispersion curves of potassium are given in Fig. E9.

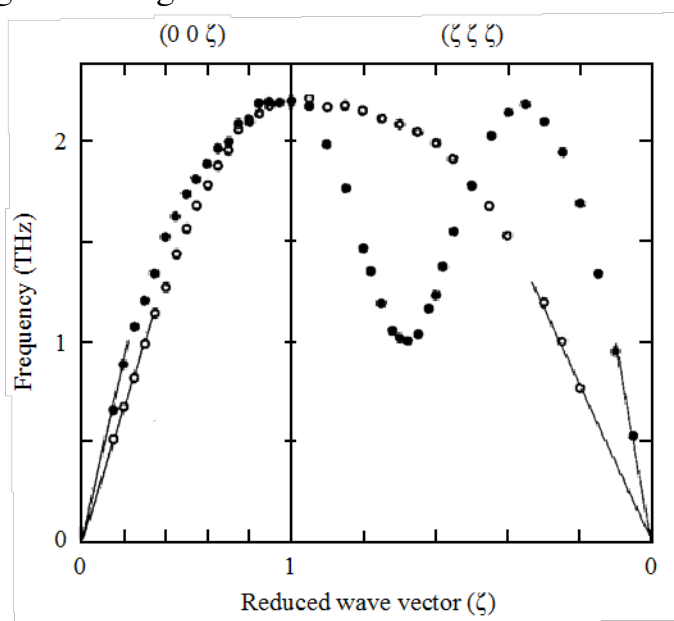


Figure E5. *Acoustic mode dispersion curves for potassium (bcc) measured by inelastic neutron scattering. (Data taken from Cowley et al. Phys. Rev. **15**, 487, 1966.)*

F. High resolution spectroscopy **(TOF, backscattering and Spin-Echo)**

The aim of this section is to get a feeling for the energy resolutions of different spectrometer types: backscattering at a pulsed and reactor source, time-of-flight chopper spectrometers (direct geometry), spin echo (NSE) spectrometers. In all the following calculations, unless said otherwise, you are to assume a neutron wavelength of $\lambda=6.27 \text{ \AA}$ which corresponds to the analysing energy of Si(111) crystals which are commonly used for high resolution inverted geometry spectrometers. Remember that Planck's constant is $h=6.6225 \times 10^{-34} \text{ Js}$, sometimes usefully expressed as $h = 4.136 \text{ \mu eV.ns}$. Neutron mass $m_n=1.675 \times 10^{-27} \text{ kg}$. In this exercise we will consider building a high resolution spectrometer which aims to have an energy resolution ΔE of 1 \mu eV . With such an instrument you will be able to see what atoms do at timescales of the order of 1 ns (rotations of molecular groups, diffusion of molecules, etc...).

For all spectrometers, different contributions add to the resolution. Typically we talk of contributions to the primary spectrometer (before the sample) and to the secondary (after the sample).

F1. Time of flight spectrometers (inverted and direct)

All contributions to the energy resolution in time-of-flight spectrometers can be formulated as an uncertainty in time $\Delta t/t$. Let's consider only the primary spectrometer (before sample) and aim for an energy resolution of 1 \mu eV .

- (i) Show first that $\Delta E/E = 2\Delta t/t$ (express E as a function of v and assume uncertainty in length is zero).
- (ii) If we want to achieve an energy resolution of 1 \mu eV , what is $\Delta E/E$?

Thinking back to the spectrometer that we have just seen in the previous exercise, it is an inverted geometry spectrometer at a time of flight source. In this type of instrument, the main contribution to the primary spectrometer comes from the moderator pulse width at a given energy. For IRIS at 6.68 \AA , the pulse width is 120 \mu s .

- (iii) Could IRIS ever achieve a resolution of 1ueV at its current length?
 [Hint: what is the contribution of the primary to IRIS in its current set-up]

Let us now consider other contributions to the neutron flight time uncertainty Δt important to time of flight spectrometers. Consider such an instrument with two choppers, CH₁ and CH₂ separated by a length L as sketched in the Figure F1a and let's first look at neutrons of $\lambda=6.27\text{\AA}$ flying parallel to z .

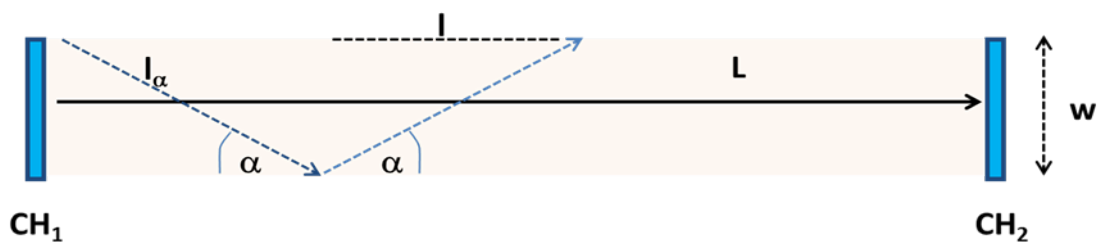


Figure F1a. Time-of-flight spectrometer with two choppers CH₁ and CH₂ separated by a distance L . Neutrons are transported through a guide of $m = 2$ coating and width w . The critical angle $\alpha = 0.1^\circ m\lambda$.

- (iv) Calculate the *allowed flight time uncertainty* along L if $L = 100\text{m}$ (Calculate the flight time), Δt . [note the value of $\Delta t/t$]
- (v) Calculate the *flight path difference* through the guide for the reflected neutrons (calculate the flight path difference with respect to neutrons which fly parallel), ΔL . [note the value of $\Delta t/t$]
- (vi) Another contribution to the time uncertainty (and thus the energy resolution) is the chopper opening time which leads to a spread in neutron velocity. Assume that CH₁ releases at $t = 0$ an arbitrarily sharp pulse, then the CH₂ delay time t_{CH_2} selects a neutron velocity v and the CH₂ opening time determines $\Delta v/v$. Calculate the *chopper opening time* for CH₂ to match the desired energy resolution of 1ueV, Δt_{CH_2} .

Mechanically, the chopper opening time is defined as $\Delta t_{\text{CH}_2} = (\beta/360)/f$, where β is the chopper window angular opening and $(\beta/360)$ is called the duty cycle which equals the fraction of neutrons transmitted by the chopper. A typical value of the duty cycle is 0.01. Calculate the *chopper frequency* needed to achieve the chopper opening time calculated before.

This condition becomes more restrictive if we consider the finite opening time of the first chopper as well. Finally, we mention that all the contributions in the primary and secondary spectrometer have to be added in quadrature:

$$\Delta t/t = \text{sqrt}[(\Delta t_1/t_1)^2 + (\Delta t_2/t_2)^2 + \dots]$$

What you can see from this exercise is that for high energy resolution, time of flight spectrometers typically require technically demanding (fast moving) choppers, long (and expensive) neutron guides and a narrow chopper windows which leads to loss in flux. At reactor facilities time of flight instruments so-called chopper spectrometers achieve resolutions of $> 10 \mu\text{eV}$. For example IN5 at the ILL at 6.3 \AA has roughly $40 \mu\text{eV}$ energy resolution. Time of flight backscattering spectrometers at pulsed sources, also require long lengths of guide if you want the high resolutions or you can reduce your pulse width using a so-called pulse shaping chopper, but a large loss in incident flux. Currently IRIS with PG002 can achieve $17.5 \mu\text{eV}$, but BASIS for example at the SNS, which is 84m can achieve $3.5 \mu\text{eV}$ with Si(111) crystals.

F2. – Crystal analyser spectrometers

In the next part of the exercise we will consider the contribution to the resolution of the secondary spectrometer for the case of a crystal analyser instrument, a backscattering spectrometer. In such spectrometers, high energy resolution is achieved by choosing Bragg angles θ as close as possible to 90° . Two major terms contribute to the energy resolution: the spread in the lattice spacing of the analyzing crystal $\Delta d/d$ and the deviation from perfect backscattering direction.

(vii) Show first that $\Delta E/E = 2\Delta\lambda/\lambda$ (express λ as a function of ν differentiate in energy).

(viii) Show that $\Delta\lambda/\lambda = \Delta d/d + \cot \theta \cdot \Delta\theta$ and discuss why we use the backscattering condition.

The first contribution to the energy resolution is $\Delta d/d = \Delta\tau/\tau$ which can be calculated by dynamical scattering theory. The second one, the angular deviation, can for $\theta \approx 90^\circ$ be expanded in powers of θ and contributes approximately as $\Delta\lambda/\lambda \sim \Delta\theta^2/8$ ($\Delta\theta$ in radians).

- (a) Calculate the first contribution to the energy resolution for a Si(111) analyser which reflects neutrons of 6.27\AA , for which $\Delta d/d = 1.86 \times 10^{-5}$. What would it be for PG(002) at IRIS (which reflects neutrons of 6.68\AA), for which $\Delta d/d = 2.0 \times 10^{-3}$?
- (b) Calculate the contribution to the energy resolution due to the deviation from backscattering for a Si(111) analyser where the sample diameter of 4cm positioned at 1.64m from the analyser.

F3. - Neutron spin-echo spectrometers

In neutron spin echo one uses the neutron spin which undergoes precessions in a magnetic field B . The precession angle φ after a path length L depends on the field integral, given by $\varphi = \gamma BL/v_n$ (γ = gyromagnetic ratio of the neutron, v_n =neutron speed). For a polychromatic beam the precession angles of the neutron spins will be very different depending on the neutron speed and thus a previously polarized beam becomes depolarized. The trick is then to send the neutrons after the sample through a field with opposite sign and with the same field integral. Therefore, for elastic scattering, the precessions are “turned backwards”, again depending on the neutron velocity, and the full polarization is recovered. This allows the use of a wide wavelength band (range of incident neutron speeds) and therefore a high intensity which is ‘decoupled’ from the energy resolution. In order to estimate a typically achievable energy resolution, we can calculate the longest time which is easily accessible in NSE which is given by $t_{\text{NSE}} = \hbar\gamma BL/(m_n v_n^3)$.

- (ix) Calculate the longest NSE achievable time for 6.27\AA neutrons assuming a field integral BL of 0.25 Tm and $\gamma = 1.832 \times 10^8\text{ T}^{-1}\text{s}^{-1}$.
- (x) What is the energy resolution achievable then by multiplying its reciprocal value with $h=4.136\text{eV}\cdot\text{ns}$.
- (xi) The longest NSE time depends on wavelength λ^3 so we could improve the resolution improves fast for increasing λ . But what are the disadvantages of this?

G. Small Angle Scattering

G1

The SANS data from 1, 5 and 10 mg/ml samples of Green fluorescent protein (Gfp) from the jelly fish *Aequorea victoria* in D₂O buffer solutions is shown below.

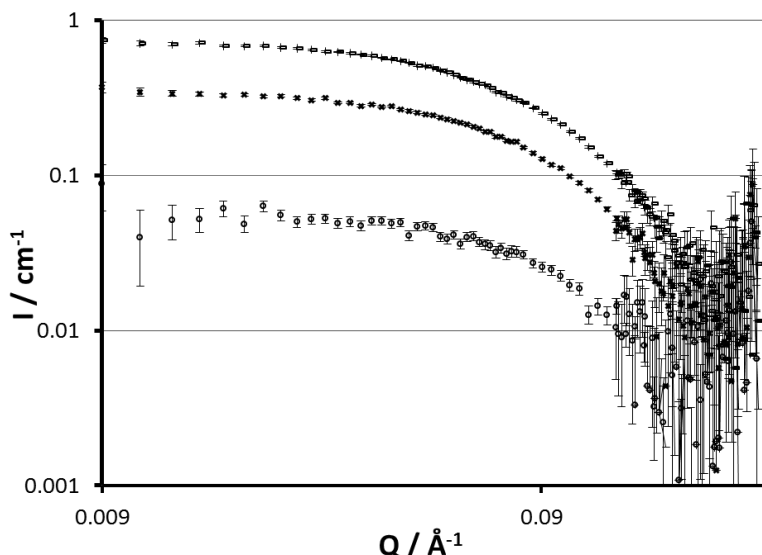


Figure G1. *Small Angle Neutron scattering Data from a solution of Green Fluorescent protein at a concentration of 1, 5 and 10 mg/ml in a D₂O buffer solution.*

(a) Using the fit of the Guinier region of the data (shown below) for the 10 mg/ml sample determine the radius of gyration (R_G).

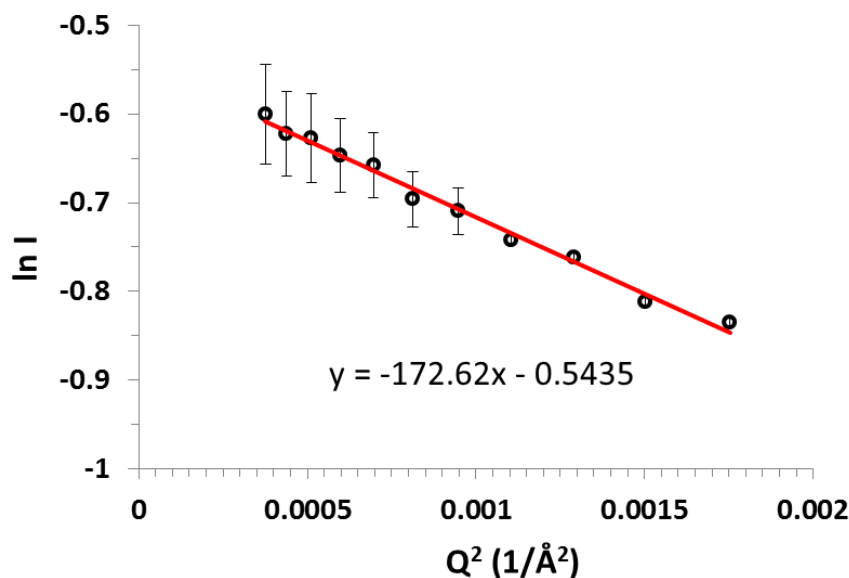


Figure G2. *Analysis of the Guinier region of the SANS data for a 10 mg/ml sample of Gfp. Circles indicate experimental data and the line indicates the fit to this data which gives the gradient shown.*

(b) The Gfp sample was collected at 3 different protein concentrations, being 1 mg/ml, 5 mg/ml and 10 mg/ml. Why was this done?

G2.

Lipid nanodiscs are formed from a bilayer of a phospholipid such as DMPC, surrounded by a belt of the poly(styrene-alt-maleic acid) copolymer with the structures shown below.

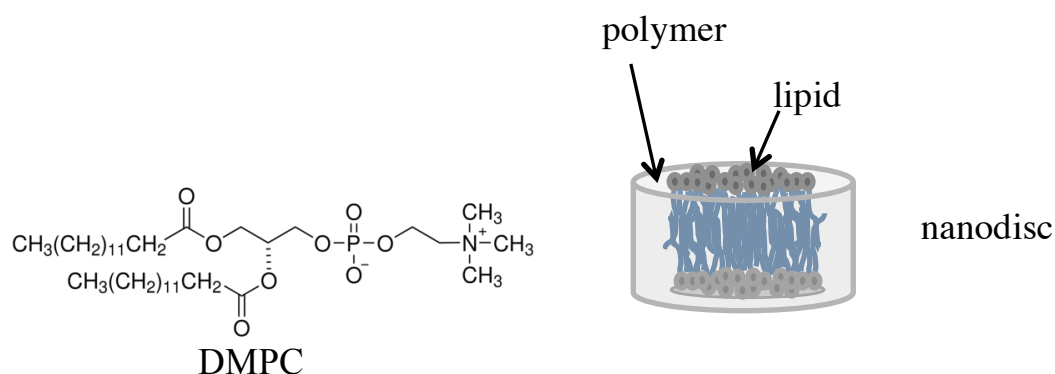


Figure G3. The Structure of 1,2-dimyristoyl-*sn*-glycero-3-phosphocholine (DMPC) and a lipid nanodisc.

a) (i) Poly(styrene-alt-maleic acid) (structural formula is below) is a strictly alternating copolymer. Calculate the scattering length density of the polymer, if the density of the polymer at 25°C is 1.27 g cm⁻³.

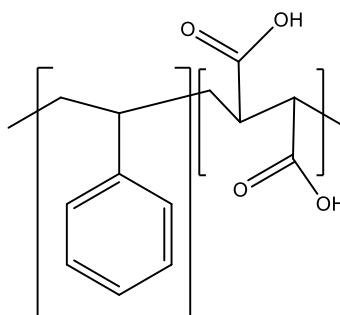


Figure G4, Poly(styrene-alt-maleic acid).

$$b(C) = 6.65 \times 10^{-13} \text{ cm}$$

$$b(O) = 5.803 \times 10^{-13} \text{ cm}$$

$$b(H) = -3.742 \times 10^{-13} \text{ cm}$$

ii) In which solvent would you see the strongest scattering signal from the polymer, H₂O or D₂O? Why?

The scattering length density of H₂O is $-0.562 \times 10^{10} \text{ cm}^{-2}$.

The scattering length density of D₂O is $6.34 \times 10^{10} \text{ cm}^{-2}$.

b) Theoretically the scattering length density of the phospholipid tails can be approximated to be the same as that of tetradecane. Calculate the scattering length density of fully deuterated tetradecane (density 0.765 g cm^{-3})

$$b(D) = 6.674 \times 10^{-13} \text{ cm}$$

$$b(C) = 6.65 \times 10^{-13} \text{ cm}$$

In a SANS experiment the core of the nanodiscs was found to be contrast matched at 78mol% D₂O/22mol% H₂O.

c) (i) A scattering pattern from the nanodiscs in 78% D₂O solution was measured. What part of the structure is responsible for the observed scattering?

(ii) What does the contrast match point of the nanodiscs core reveal about the actual structure of the nanodiscs?

The scattering length density of H₂O is $-0.562 \times 10^{10} \text{ cm}^{-2}$.

The scattering length density of D₂O is $6.34 \times 10^{10} \text{ cm}^{-2}$.

d)

(i) at higher temperatures the nanodiscs restructure to form spherical unilamellar vesicles with radii in the micron range. Sketch the small angle scattering curve expected for this new structure on a logI vs logQ plot.

(ii) In concentrated solutions the nanodiscs stack to form long cylindrical strings of discs with a uniform spacing between the discs. These strings align vertically in the sample cell. Sketch the expected scattering pattern seen on the 2D detector.

(iii) Membrane proteins have hydrophilic ends and a hydrophobic middle so prefer to sit in a lipid bilayer so that only the hydrophilic parts are exposed to water. A membrane protein was added to each nanodisc. What experiments would you need to do to best understand the scattering from this system? How might you model the scattering from this system?

e) For very anisotropic particles, e.g. discs, the Guinier approximation, which assumes spheres, is no longer strictly correct. A similar approximation can be derived using the form factor for a disc which gives the linearised equation:

$$\ln(Q^2 I_c(Q)) = -Q^2 R_t^2 / 12 - \ln A \quad \text{where } R_t \text{ is the thickness of the disc.}$$

The scattering from a solution of nanodiscs is plotted on a graph of $\ln(Q^2 I)$ vs Q^2 . The slope of the graph is 121 \AA^2 . What is the thickness of the nanodiscs? What assumption have you made to calculate this?

H. Reflectometry

H1) You are writing an experimental proposal and you wish to simulate a polarised neutron reflectivity (PNR) curve. To work out what thickness of material is best to use for magnetic contrast matching, this can then be grown in the lab sputter growth chamber. You are using a nonmagnetic substrate of silicon dioxide (SiO_2) to support a magnetic reference layer in this case Nickel (Ni).

a. Calculate the SLD in units of $\times 10^{-6} \text{ \AA}^{-2}$ for SiO_2 given:

Density of SiO_2 is 2533 kgm^{-3} ,

$b(\text{Si}) = 4.1491 \text{ fm}$,

$b(\text{O}) = 5.803 \text{ fm}$

Molar mass Si = $28.0855 \text{ g mol}^{-1}$

Molar mass O = $15.999 \text{ g mol}^{-1}$

Avogadro's number $N_a = 6.022 \times 10^{23}$ atoms per mole

b. Calculate the structural SLD for Ni in units of $\times 10^{-6} \text{ \AA}^{-2}$ given:

Density of Ni is 8908 kgm^{-3} ,

$b(\text{Ni}) = 10.3 \text{ fm}$

Molar mass $M_w = 58.6934 \text{ g mol}^{-1}$

c. Calculate the magnetic SLD for Ni in units of $\times 10^{-6} \text{ \AA}^{-2}$ given:

Magnetic Moment of Ni $m = 1.8 \mu_B$ per atom

d. Calculate the total SLD values for both polarised neutron spin states of Ni in units of $\times 10^{-6} \text{ \AA}^{-2}$?

H2) All simulations as well as any data should be calculated/collected in terms of wave vector transfer \mathbf{Q} .

a) Why is this a good thing to do?

b) Derive an expression for \mathbf{Q}_z starting from the momentum transfer equation and assuming elastic scattering in terms of λ and θ .

$$\mathbf{Q} = \mathbf{k}_i - \mathbf{k}_f$$

H3) You now want to check there is sufficient difference between the two polarised spin states of reflectivity for the SiO_2/Ni sample, the easiest way to do this is to calculate the critical edge position.

a) Given:

$$n^2 \approx 1 - \frac{Nb\lambda^2}{\pi} (*)$$

(To see where this originates see Chapter 4 of D. S. Sivia “Elementary Scattering Theory”)

Derive an expression from basic principles for the critical angle Q_c ?

b) Calculate Q_c for both polarised spin states for a Ni/Air interface (arb thickness) monolayer sample.

c) What does the difference between the spin up and spin down Q_c values give a direct measure of?

H4) Silicon ($SLD_{Si} = 2.07 \times 10^{-6} \text{ \AA}^{-2}$) and Bismuth ($SLD_{Bi} = 2.404 \times 10^{-6} \text{ \AA}^{-2}$) have very similar SLD's. Why is it a bad idea in neutron reflectivity to use Bi as a reference layer on a Si substrate, what does it do to the data?

H5) You have some old neutron reflectivity data and you want to use it to calibrate the growth rates of the sputter guns in your sputter system.

a) Using Braggs Law obtain the approximate thickness from the following data set (see figure H1): work out the thickness based on the four sets of ΔQ (peak to peak distance in Q).

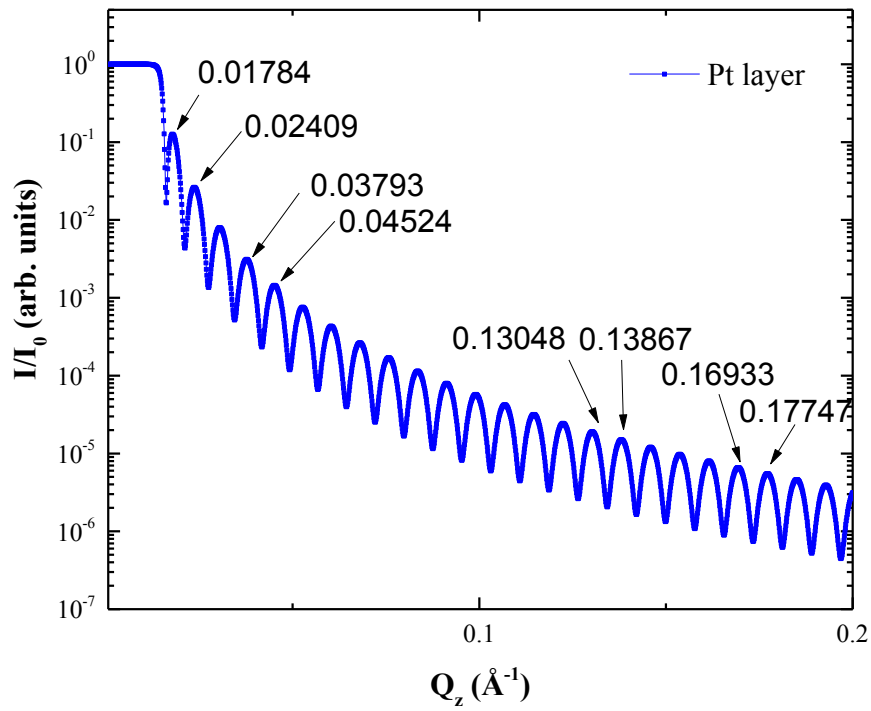


Figure H1, Neutron reflectometry data.

- b) Why do the numbers for the thickness of the layer vary?
- c) Which region should always therefore take the difference of two fringes from and what is the best estimate of the thickness of the film?

I: Polarized Neutrons

- I1.** a) A measurement of a Si Bragg peak using the instrument in Fig. I1, give 51402 counts/second with the flipper off and 1903 counts per second with the flipper on? What is: a) the Flipping Ratio, and b) the beam polarization? Provide also a calculation of the experimental uncertainty in these values.

b) What would be the main sources of systematic error in this measurement?

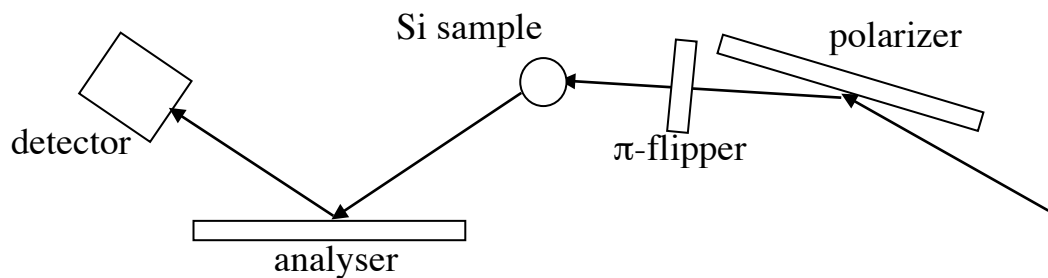


Figure H1. *Schematic polarization analysis instrument*

- I2.** a) Fig. I2 shows a configuration for a Dabbs'-foil (current sheet) flipper, designed for neutrons of wavelength 2 \AA . A current I flows vertically along the foil, giving rise to a horizontal field $B_F = 3 \text{ mT}$. The overall guide field B_G – also equal to 3 mT – is cancelled at the foil position by correction coils. The overall distance between the purely vertical guide field regions is 20 cm .

Transport of the neutron polarization is said to be adiabatic if then ratio between the neutron Larmor precession frequency $\omega_L = \gamma B$ and the field rotation frequency is greater than 10. In this limit the neutron polarization will be efficiently transported. By checking the rate of the field rotation, state whether you believe that this is a good design for a π -flipper.

The neutron gyromagnetic ratio, γ_n , is the ratio of the neutron magnetic moment to its angular momentum, i.e.: $\gamma_n = \mu_n / \frac{1}{2}\hbar = 1.832 \times 10^8 \text{ rad. s}^{-1} \text{ T}^{-1}$

- b) Suggest ways in which the design may be improved.

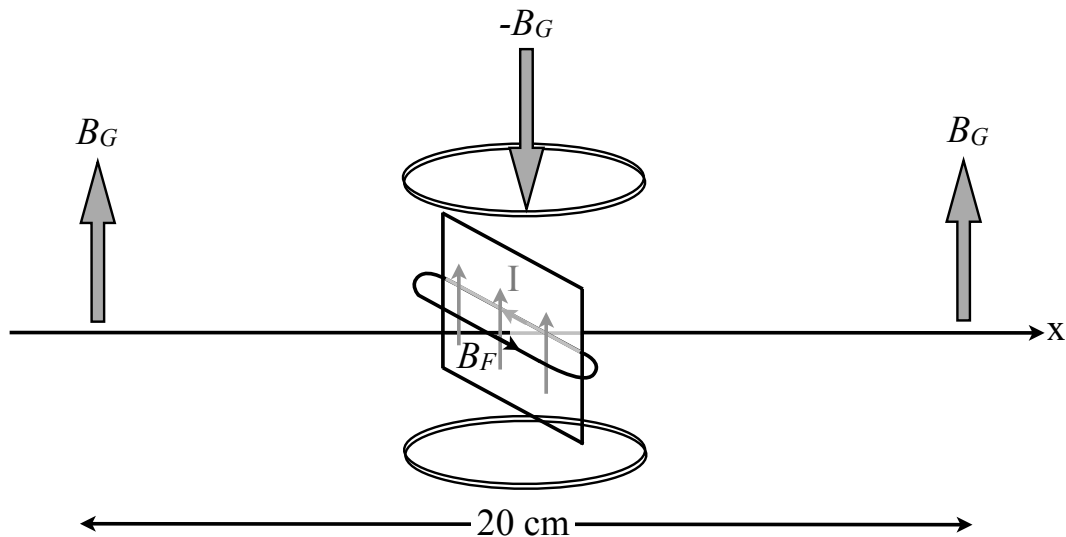


Figure I2: Design for a Dabbs' Foil π -Flipper

- I3.** a) Show that the polarizing efficiency of a crystal monochromator is given by

$$P = \frac{2F_N F_M}{F_N^2 + F_M^2},$$

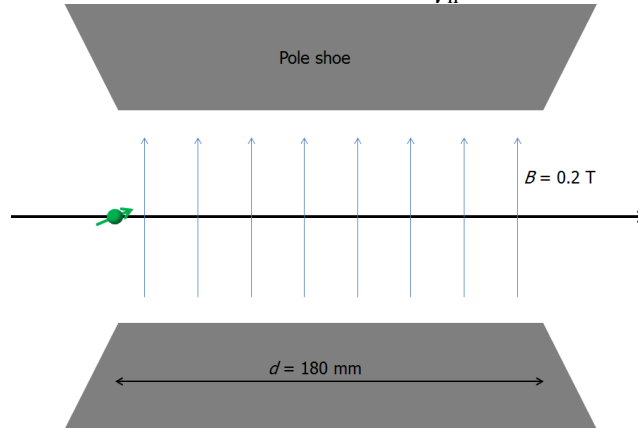
where the symbols have their usual meanings.

- b) By expressing the polarization as a function of the ratio of structure factors, show that the maximum polarization is obtained when the nuclear and magnetic structure factors are equal in magnitude.

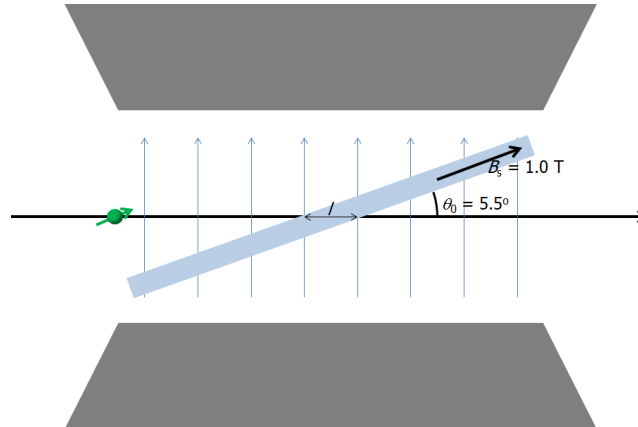
- I4.** Why is it not necessary to analyse the neutron spin when scattering from a ferromagnet saturated in a direction perpendicular to Q ?

J. Spin-Echo Small-Angle Neutron Scattering

J1) The SESANS instrument in Delft has four electromagnets creating the Larmor precession of the neutrons traversing their magnetic fields. The precession angle ϕ of polarised neutrons with a wavelength λ in a magnetic field with a strength B and a length d is $\phi = \frac{\gamma_n m \lambda d B}{h}$. The magnets have a length of 180 mm in the direction of the neutron path and can have a maximum field of 0.2 T. The gyromagnetic ratio of the neutron has a value of $\gamma_n = 1.832 \times 10^8 \text{ rad s}^{-1} \text{ T}^{-1}$.

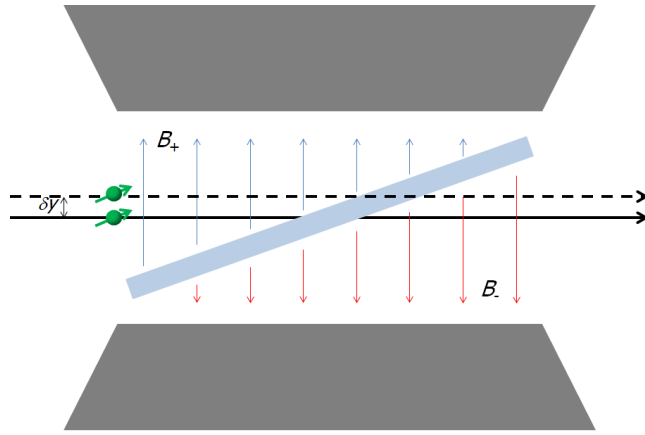


1. Calculate the maximum number of precessions for neutrons with a wavelength of 2 \AA in one of these magnets.



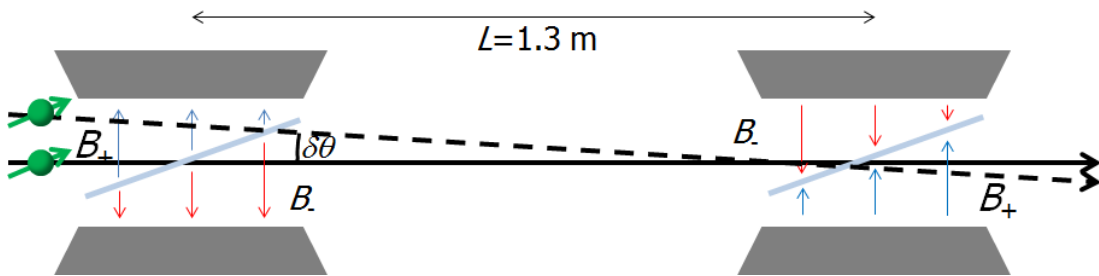
For the SESANS instrument in Delft a thin foil is used as π -flipper (see the figure above). The magnetic field of a thin magnetic film will be in the plane, as shown in the figure. The saturation magnetic field of the permalloy (20% Fe, 80% Ni) film is 1.0 T. The foil is tilted over an angle of $\theta_0 = 5.5^\circ$ with respect to the horizontal plane. The neutron will precess over the length l , while it travels through the foil.

2. Calculate the thickness of the foil to produce a π -flip.



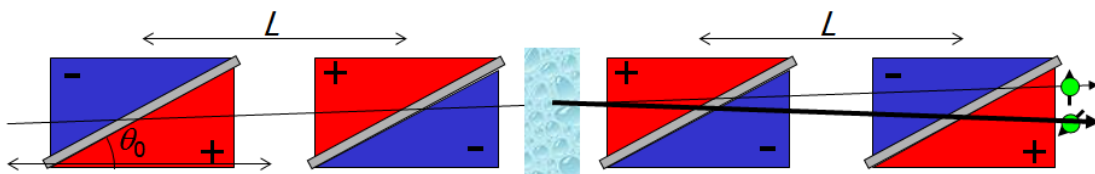
One can consider the Larmor precession after the π -flipper as being reversed. We assume that a spin-echo instrument is sensitive to a tenth of a precession ($2\pi/10$ radian). This is a reasonable assumption since the polarisation will then decrease from 1.00 to $\cos(2\pi/10) = 0.81$. We consider now the precession through only one magnet at its maximum field of 0.2 T with a magnetised foil flipper as depicted in the figure above.

3. Calculate the sensitivity one achieves for the height of a horizontal neutron path through this electromagnet.



We now consider two of these magnets separated over a length of 1.3 m with the main fields in the same direction as depicted in the figure above.

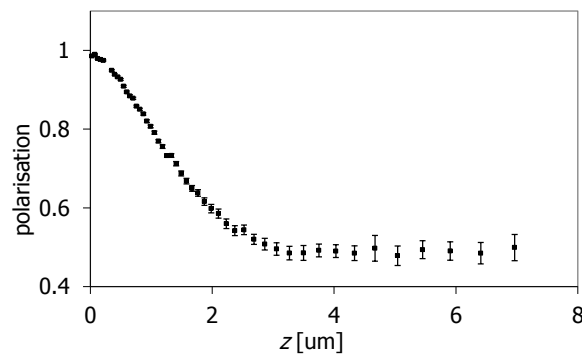
4. Calculate the sensitivity one achieves for the vertical angle with respect to the optical axis
5. In the small-angle approximation the wave-vector transfer Q is given by $Q = 2\pi\theta / \lambda$, in which θ is the total scattering angle. The spin-echo length δ can be defined by the relation between the Larmor precession caused by the wave-vector transfer $\varphi = \delta Q$. Experimentally the spin-echo length is determined by the wavelength λ , the tilt angle of the foils θ_0 , the distance between the two magnets in one arm L and the applied magnetic field B .



Derive the following relation for the spin-echo length:
$$\delta = \frac{\gamma_n m \lambda^2 L B \cot \theta_0}{\pi h}$$

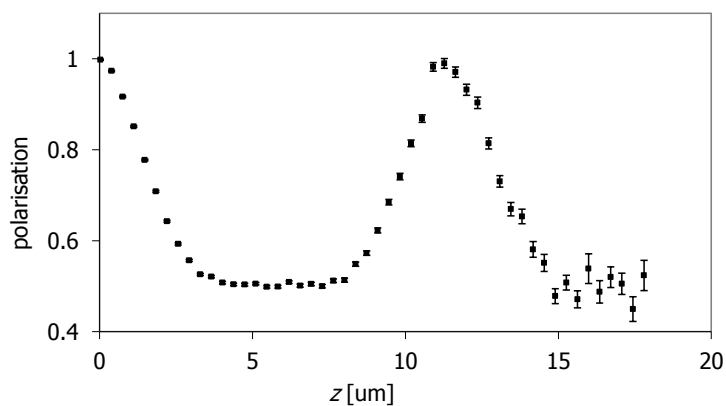
J2) The polarisation in SESANS is $P(\delta) = \exp\{\Sigma_t[G(\delta) - 1]\}$, where Σ_t is the average number of times a neutron scatters, when traversing the sample, i.e. this takes into account multiple scattering and $G(\delta)$ is the scattering length density correlation function projected along the neutron propagation axis. For a two phase system the scattering power becomes $\Sigma_t = \lambda^2 t (\Delta\rho)^2 \phi(1 - \phi)\xi$, where t is the sample thickness, λ is the neutron wavelength, $\Delta\rho$ is the neutron scattering length density contrast, ϕ the volume fraction of one the phases and ξ the correlation length of the scattering system (for anisotropic systems along the direction of the neutron beam). For more details see [R. Andersson *et al.* J. Appl. Cryst. 41, 868-885 (2008)].

1. For a solid sphere with radius R the projected correlation function can be well approximated by a Gaussian: $G(\delta) = \exp[-(9/8)(\delta/R)^2]$ with a correlation length $\xi = 3R/2$. In the graph below a measurement of a colloidal dispersion of latex spheres is shown.



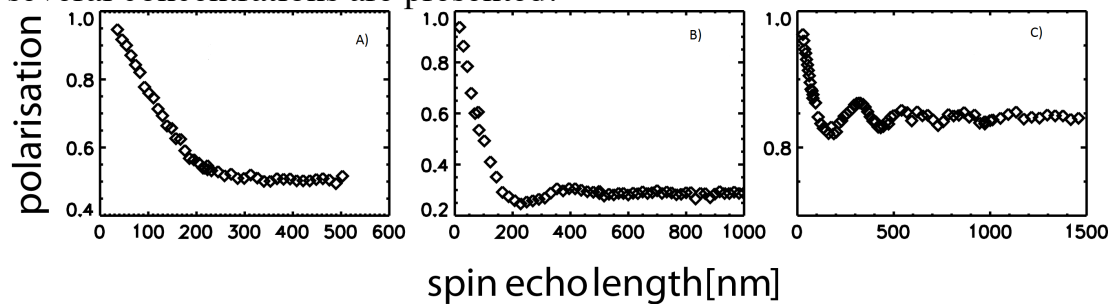
The measurements were performed with a wavelength of $\lambda = 2.1 \text{ \AA}$, a sample thickness of 5 mm and the scattering length density contrast is $\Delta\rho = 1.3 \times 10^{14} \text{ m}^{-2}$. Derive from the measurement the radius R of the spheres and the volume fraction ϕ .

2. In the graph below a measurement on a silicon photo etched grating is presented.



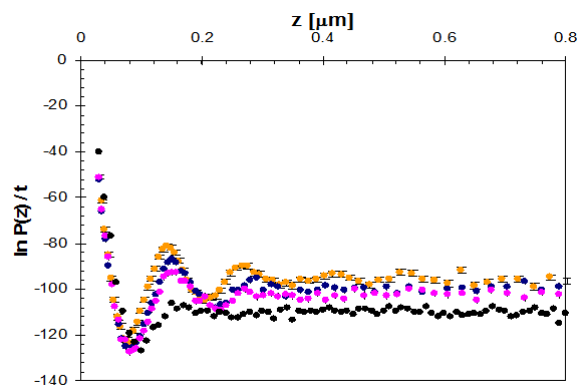
The scattering length density of silicon is $\Delta\rho = 2.07 \times 10^{14} \text{ m}^{-2}$. Derive from the measurement the period of the grating, the trench width and the depth of the trenches.

3. In the graph below three measurements on dispersions of silica spheres at several concentrations are presented.



Determine which of the graphs A), B) and C) contain, respectively, a 0.56 volume fraction in a cell with a thickness of 1 mm, a 0.23 volume fraction with a thickness of 2 mm and a 0.055 volume fraction with a thickness of 10 mm and motivate your answer.

4. In the graph below measurements on dispersion of charged polystyrene colloids in different salt concentrations are presented. Please note that on the vertical axis the logarithm of the polarisation divided by the sample thickness is plotted to combine the results of different thickness'.



Motivate how the signal is going from low to high salt concentration in this graph.

K. Magnetic Neutron Scattering

K1.

Using the convolution theorem, derive the expression for the convolution of two Gaussian functions

$$f(x) = \frac{1}{\sqrt{2\pi\sigma^2}} \exp\left(-\frac{x^2}{2\sigma^2}\right)$$

given that the Fourier transform of a Gaussian is also a Gaussian of reciprocal width

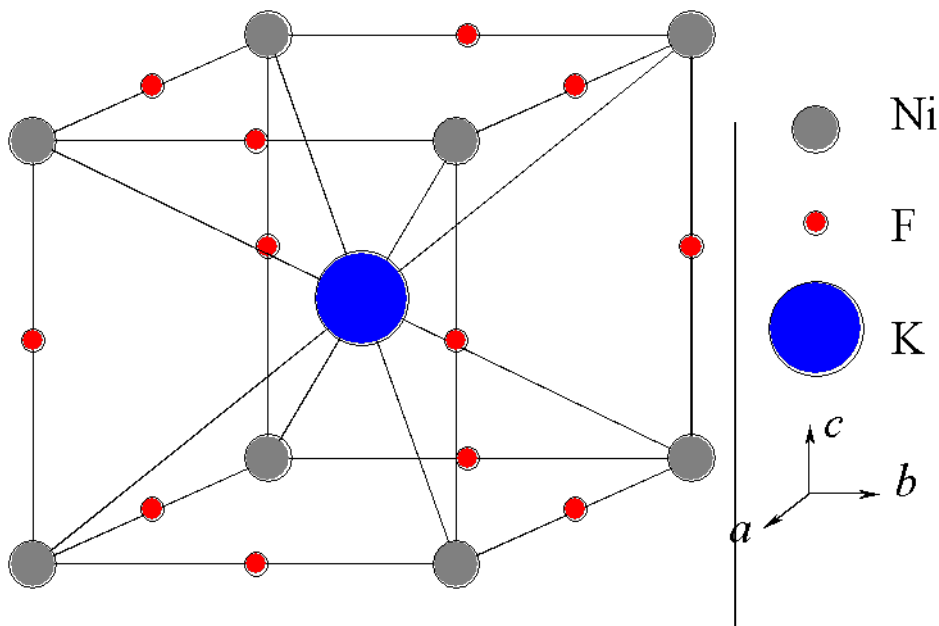


Figure K1: *The cubic perovskite structure of KNiF_3*

K2. KNiF_3 has a cubic perovskite structure, shown in Figure K1. It becomes antiferromagnetic below a Néel temperature of $T_N = 275$ K. In this magnetic structure, the magnetic ions are the Ni ions, whose magnetic moments lie along the edges of the cube. Each moment is antiferromagnetically coupled to its nearest neighbour.

Start by assuming that the material has a single magnetic domain and that the magnetic moments point along c .

2.1 Draw the magnetic unit cell in real space.

2.2 Draw the nuclear reciprocal lattice plane spanned by $[110], [001]$ from $-2 \leq h, k, l \leq 2$

2.3 Superimpose on this the magnetic reciprocal lattice. Index the magnetic points with the magnetic reciprocal lattice units.

2.4 Write the magnetic structure factor for the magnetic peaks. Will all the peaks have the same intensity? If not, why not? What implication does this have for the symmetry of the magnetic lattice?

K3. KNiF_3 is said to be an excellent example of a Heisenberg antiferromagnet. This means that it will have almost no anisotropy and the spin waves between the Brillouin zone centres will resemble something like in figure K2.

Assume that the spin waves can be described using a classical picture (i.e. magnetic moments precessing on cones). Identify the Brillouin zone centres along the $[001]$ and $[110]$ axes. Will spin waves be measurable along these directions? If yes, how will the intensities compare?

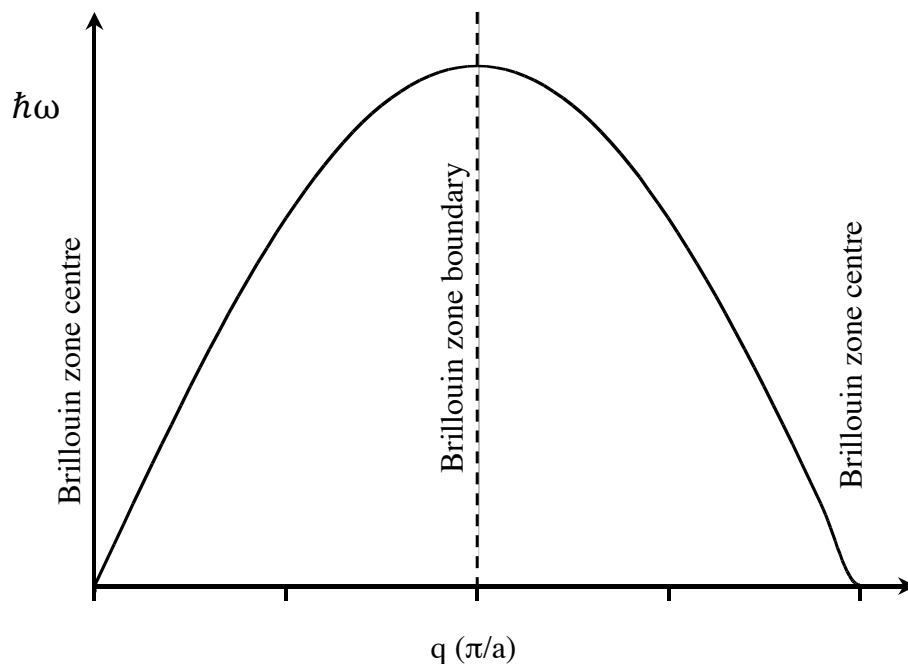


Figure K2: Schematic showing a spin wave dispersion from a Heisenberg antiferromagnet.

K4. Now assume that the sample has many domains. What will happen to the intensities of the Bragg peaks and the inelastic scattering?

L. Chemical Applications

L1: Incomplete exchange of H₂O and D₂O

When we perform experiments to study the adsorption of molecules on a solid surface from a liquid we need to change the scattering length density of the liquid to help us solve the adsorbed layer structure. However, it is often not easy to completely exchange the solutions and be sure we have moved from one isotopic mix to another. However, the position of the critical edge can be very helpful in identifying if we have exchanged enough or not...as this example demonstrates:

- (a) Using the data in the table below calculate the Scattering Length Densities of H₂O and D₂O.
- (b) Calculate the neutron refractive indices for Si, H₂O and D₂O for a neutron of wavelength 1.8 Å (1.8x10⁻¹⁰m).
- (c) Calculate the critical angle you would expect for a neutron beam of wavelength 1.8 Å (1.8x10⁻¹⁰m) passing from silicon to D₂O.
- (d) The critical edge for reflection from a silicon block in water that should be D₂O is experimentally determined to be 0.1 degrees.
This sample was prepared by exchanging H₂O for D₂O.. But not all the H₂O was removed. How much H₂O was left in the cell? (% v/v)?

Isotope	Scattering length	Atomic mass (g/mol)	Scattering length density
H	-3.74x10 ⁻¹⁵ m	1	
D	+6.671 x10 ⁻¹⁵ m	2	
O	+5.803 x10 ⁻¹⁵ m	16	
Si			2.07x10 ⁻⁶ Å ⁻²

Hint #1: Calculate the volume of one water molecule? (What is the mass of one mole of water? What is the volume of one mole of water? hence find the volume of one molecule). What is the relative volume of one molecule of H₂O and one of D₂O (why?)?

Hint #2: What is the scattering length of one molecule of (a) H₂O and (b) D₂O?

Hence find the scattering length densities of H₂O and D₂O (-0.56 and 6.40 x10⁻⁶ Å⁻²).

Hint #3: Refractive index, n_i , is given by: $n_i = 1 - Nb\left(\frac{\lambda^2}{2\pi}\right)$. $\frac{\lambda^2}{2\pi} = 0.5156$.
 Nb is the scattering length density of phase i .

Hint #4: Relation of refractive indices to reflected angles in phases 0 and 1 are:

$$\frac{n_1}{n_0} = \frac{\cos \theta_0}{\cos \theta_1}$$

When one is at the critical edge $\theta_1 \rightarrow 0$ and $\cos \theta_1 \rightarrow 1$.

Can you find the refractive index of the ‘water’?

Can you find the scattering length density of the water?

How much H_2O and D_2O would you need to make water of this composition?

L2 Incoherent neutron data can be used to see how much of a material is adsorbed on a surface using ‘Dynamic contrast’. A molecule that is stuck to a solid surface doesn’t move much, while if it is in solution it can diffuse a lot. Figure (a) shows how we get a plateau in the measured elastic intensity if a solid monolayer forms of the surface where the height of the plateau tells us how much of the species is present on the surface.

The figure (b) below gives an example of some elastic incoherent scattering as a function of temperature for octane and decane mixtures: Note that the level of the plateau falls on addition of decane.

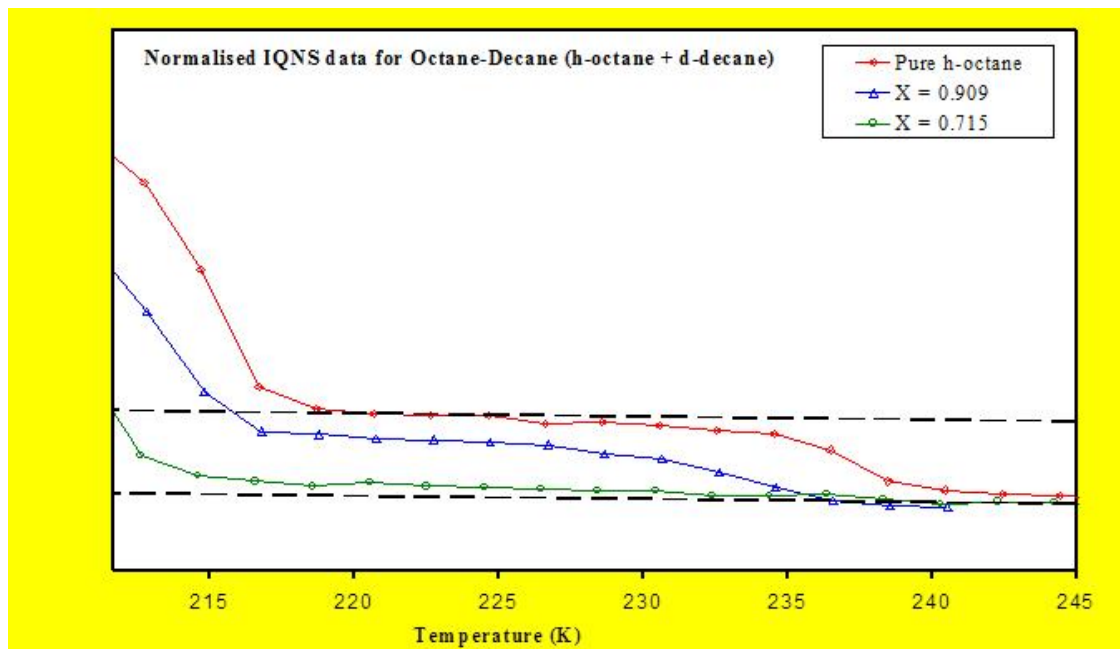


Figure L1

- (a) Explain why the plateau level falls as we add decane to the octane. (what isotopic combinations of octane and decane were used and why?).

(b) Using the figure L1:

- (i) estimate what fraction of the monolayer is octane when the bulk solution composition is 0.909 mole fraction octane
- (ii) Estimate the fraction of the surface is octane when the bulk composition is 0.715 mole fraction octane.
- (iii) Plot a graph of surface mole fraction of octane vs bulk mole fraction of octane: (There are also two other points on this graph you know)

Which species is preferentially adsorbed (octane or decane)?

M. Biological Applications

M1

Prior to any neutron scattering experiment it's advisable to calculate the theoretical ("dry") scattering length density (ρ) of your sample components. ρ is given by:

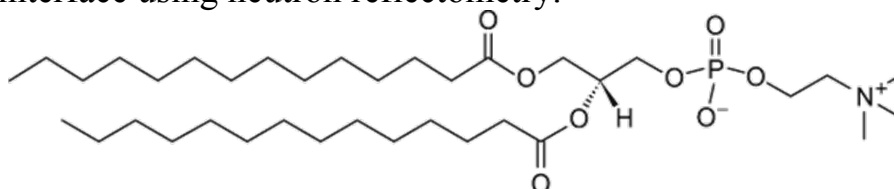
$$\rho = \frac{\sum b}{V} \quad (\text{Eq M1})$$

Where, $\sum b$ is the sum of the molecules scattering lengths and V is the molecular volume. A table of neutron scattering lengths is given below:

Table M1, Neutron scattering lengths

Element	Coherent Scattering Length (b)/ 10^{-5} \AA
Hydrogen	-3.74
Deuterium	6.671
Carbon	6.646
Nitrogen	9.36
Oxygen	5.803
Sulphur	2.847
Phosphorous	5.13

We are going to examine the structure and coverage of a DMPC bilayer at the solid/liquid interface using neutron reflectometry.



1,2-ditetradecanoyl-*sn*-glycero-3-phosphocholin (DMPC)

Molecular Formula : $C_{36}H_{72}NO_8P$

Molecular Weight : 677.933

Figure M1, DMPC.

A, from the information in tables 1 and 2 calculate the ρ 's of DMPC's head and tail regions.

Table M2, Molecular formulas and areas for DMPC's head and tail region in H_2O and D_2O :

Component/ molecule	Formula	volume / \AA^3
DMPC Tails	$C_{26}H_{54}$	771
DMPC Head group	$C_{10}H_{18}NO_8P$	304

M2.

Figure M2 gives the neutron reflectivity data, model data fits and the ρ density profiles these fits describe for a DMPC bilayer at the silicon/water interface examined in D_2O ($\rho_{D_2O} = 6.35 \times 10^{-6} \text{ \AA}^{-2}$) and H_2O ($\rho_{H_2O} = -0.56 \times 10^{-6} \text{ \AA}^{-2}$).

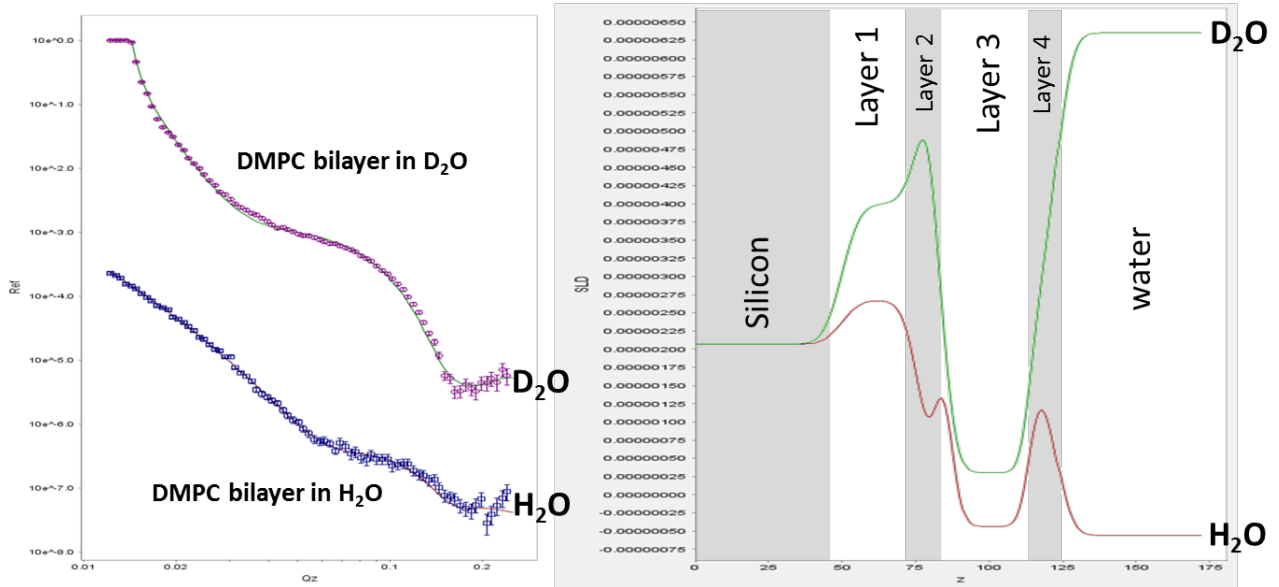


Figure M2, Neutron reflectivity profiles, model data fits and the scattering length density profiles these fits describe for a DMPC bilayer at the silicon/liquid interface examined in D_2O (top) and H_2O (bottom).

A, The structure of the DMPC bilayer has been examined under two differing solution isotopic contrasts (D_2O and H_2O).

Based on the theoretical ρ 's calculated in question M1, and the known ρ 's for D_2O and H_2O , which contrast will be most sensitive to the bilayer headgroups and which will be most sensitive to the tails?

B, In a given experiment an interfacial lipid bilayer structure was fitted with a 4 layer model to describe the interfacial structure, as shown in Table 3. Name the three lipid components and one non lipid component of the interfacial structure which were described by the 4 layers.

Table M3, Parameters obtained from fitting NR data from a DMPC bilayer deposited at the solid/liquid interface to a four layer description of the interfacial structure.

Layer	Thickness / \AA	$\rho_{\text{fitted } D_2O} / 10^{-6} \text{ \AA}^{-2}$	$\rho_{\text{fitted } H_2O} / 10^{-6} \text{ \AA}^{-2}$
1	27.4	4.04	2.62
2	5.2	2.86	1.1
3	27.6	0.17	-0.38
4	8.8	2.86	1.1

C, The fitted scattering length density of one of the bilayer layers can be used to determine the total bilayer coverage across the silicon/water interface. The fitted ρ 's of the bilayer layers are related to the theoretical ρ 's calculated in M1 by:

$$\rho_{fitted} = (\varphi_{lipid}\rho_{lipid}) + (\varphi_{water}\rho_{water}) \quad (\text{Eq M2})$$

Where ρ_{fitted} is the scattering length density value obtained from a given layer of the model data fit, φ_{lipid} and φ_{water} is the volume fractions of the lipid and water respectively within that region of the interfacial structure and ρ_{lipid} and ρ_{water} are the theoretical ρ 's calculated for these components.

Using the fitted ρ values from the D₂O contrast given in table M3 and the theoretical ρ values for your lipid and water components calculated in M1 determine suitable equation for and calculate the volume fraction of the DMPC bilayer across the silicon water interface.

Hint : You determined the D₂O contrast was especially sensitive to one component in **M2 A!**

M3

Deuterium labelling of samples can be a powerful tool in determining the contributions of individual components to a complex structure if contrast between components isn't found naturally. This type of sample labelling is often used to determine the relative contribution of individual domains in a protein complex and in lipid bilayers can be used to allow for the identification of the location of individual lipid species.

Here we will examine a model of the asymmetrical Gram negative bacterial outer membrane. The bilayer has been labelled with tail deuterated (d₆₂) DPPC (1,2-dipalmitoyl-sn-glycero-3-phosphocholine) and hydrogenous (natural abundance hydrogen) lipopolysaccharides (LPS). By examining the SLD profile of the bilayer tails determined by fitting experimental NR data we can deduce the asymmetry of the model membrane.

Firstly, we need to determine the theoretical ρ 's for our sample components, in this case the lipid tails and solution only. The ρ_{tails} of hydrogenous LPS is the same as that used for the tails of DMPC in M1, and ρ of D₂O and H₂O remain the same as used in M2. Therefore, we only need to calculate the $\rho_{d-tails}$ for tail deuterated DPPC.

A, Using the information in Table M4, determine the theoretical ρ of the deuterated DPPC tails:

Table M4, *Molecular formulas and area for DPPC's tail region:*

Component/ molecule	Formula	volume / Å ³
d-DPPC Tails	C ₃₀ D ₆₂	823

Figure 3 gives the neutron reflectometry profiles, model data fits and ρ profiles for a d-DPPC/h-LPS bilayer at the solid/liquid interface examined using three isotopic contrasts.

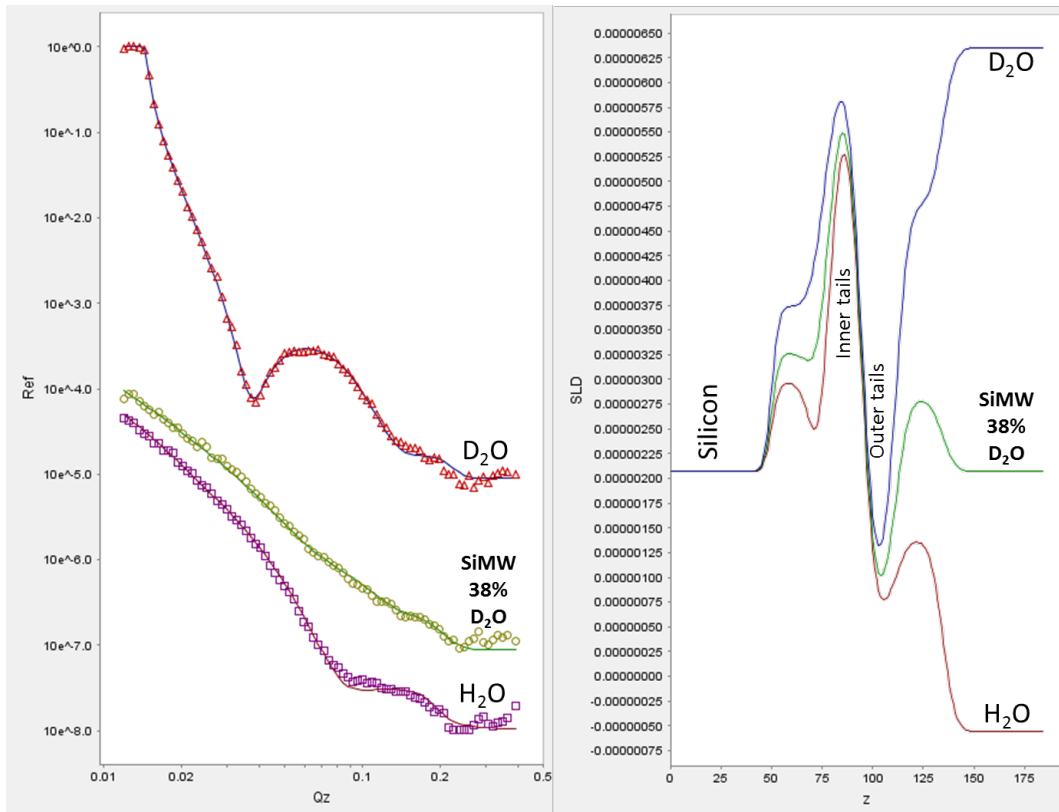


Figure M3, Neutron Reflectivity profiles, model data fits and the scattering length density profiles these fits describe for an asymmetrical DPPC/RaLPS bilayer at the Silicon/liquid interface examined in D₂O (top), silicon matched water (middle) and H₂O (bottom).

In the case of this data, the ρ_{fitted} of the tail layers of all solution isotopic contrasts is determined by:

$$\rho_{\text{fitted}} = (\varphi_{d\text{-tails}} \times \rho_{d\text{-tails}}) + (\varphi_{h\text{-tails}} \times \rho_{h\text{-tails}}) + (\varphi_{\text{water}} \times \rho_{\text{water}}) \quad (\text{Eq2})$$

The lipid tails contain no labile hydrogens therefore the only difference between the tail SLDs of the individual solution contrasts is due to the presence of water within the tail regions (due to membrane defects across the silicon surface).

B, Using the data in table M5 and the known ρ 's of H₂O and D₂O determine the φ_{water} within the bilayer inner and outer leaflets.

Table M5, Scattering length densities of the inner and outer bilayer leaflets obtained from differing H₂O and D₂O isotopic contrasts.

Layer	Thickness / Å	$\rho_{\text{fitted D2O}} / 10^{-6} \text{ \AA}^{-2}$	$\rho_{\text{fitted H2O}} / 10^{-6} \text{ \AA}^{-2}$
Inner tails	17	6.06	5.71
Outer tails	15	0.95	0.61

C, Using the theoretical ρ 's of the tails of d-DPPC and h-LPS, the fitted ρ values in table 5 and the bilayer tails hydration (determined in M3, B) determine the φ of DPPC and LPS in the inner and outer bilayer leaflets.

Hint : Only use a single fitted ρ value and remove the contribution of the solution to this to start.

N. Disordered Materials Diffraction

N1.

The interatomic potential, the pair distribution function, the coordination number, and the structure factor. (N.B. To do this exercise it is helpful to have access to a computer spreadsheet.)

Typically atomic overlap is prevented by strong repulsive forces that come into play as soon as two atoms approach one another below some characteristic separation distance σ (which is usually expressed in units of $\text{\AA} = 10^{-10}\text{m}$). At greater distances the atoms are normally attracted to one another by weak van der Waals (dispersion) forces, the magnitude of which is governed by an interaction parameter ϵ , which can be expressed in units of kJ per gm mole.

These facts can be conveniently (but only approximately) expressed by the model Lennard-Jones potential energy for two atoms separated by a distance r :

$$U(r) = 4\epsilon \left(\left(\frac{\sigma}{r} \right)^{12} - \left(\frac{\sigma}{r} \right)^6 \right) \quad (\text{N1.1})$$

The radial distribution function (RDF), normally written $g(r)$ and also called the pair distribution function (PDF), describes the relative density of atoms (compared to the bulk density) of atoms a distance r from an atom at the origin.

N1.1 The pair potential.

- With $\epsilon = 0.6\text{kJ/mole}$ and $\sigma = 3.0\text{\AA}$, sketch this function approximately in the distance range $0 - 10\text{\AA}$.
- What do the values of ϵ and σ signify?
- Mark on your graph the repulsive core and dispersive regions.

N1.2 Low density limit.

According to the theory of liquids (see for example Theory of Simple Liquids, J P Hansen and I R McDonald, 2nd Edition, Academic Press, 1986), in the limit of very low density (e.g. like the density of the air in the atmosphere), the PDF between atom pairs is given by the exact expression:

$$g_{\text{low}}(r) = \exp \left[-\frac{U(r)}{k_B T} \right] \quad (\text{N1.2})$$

where k_B is Boltzmann's constant. In the units of kJ per mole $k_B = 0.008314$ kJ/mole/K.

- Sketch this function for the Lennard-Jones potential used in N1.1 a) at (say) $T = 300\text{K}$. $g(r)$ is the primary function which is being measured in a diffraction experiment.

- b) From your sketch, describe briefly the main differences between $U(r)$ and $g(r)$.
- c) Describe qualitatively what would happen to $g_{\text{low}}(r)$ for example if you increased ϵ by a factor of 2, or increased σ by 20%?

Note that in the limit of zero density $g_{\text{low}}(r)$ does not go to zero.

N1.3 High densities.

Of course real materials occur with much higher densities than those of low density gases. This gives rise to an additional contribution to $g(r)$ from three-body and higher order correlations. In general these are difficult or impossible to calculate analytically, so that resort has to be made to computer simulation to estimate the effect of many body correlations.

Figure N1.1 shows a simulated $g(r)$ for our “Lennard-Jonesium” of N1.1, at two densities, (a) $\rho = 0.02$ and (b) $\rho = 0.035$ atoms/Å³ respectively.

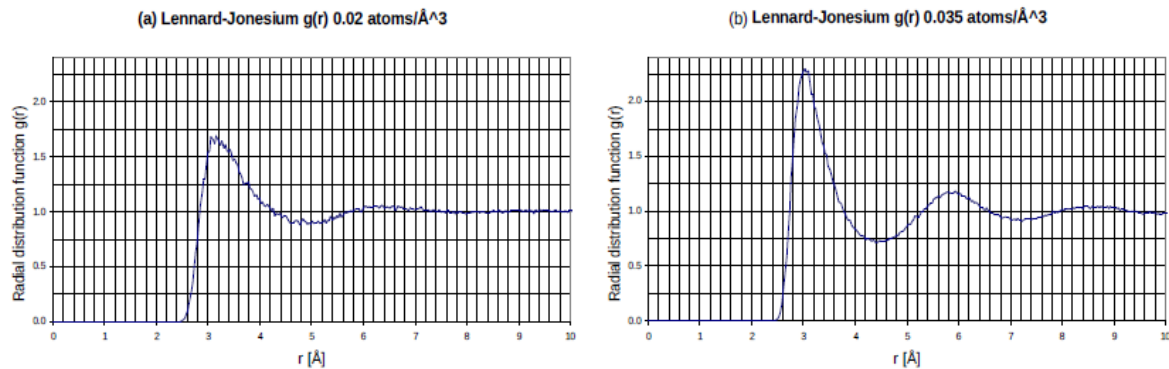


Figure N1.1

a) Comparing these with your “zero density” sketch of $g(r)$ from N1.2, describe the main effects of many-body correlations on $g(r)$. In particular:-

- How does the position of the first peak move with the change in density?
- How do the positions of the second and subsequent peaks move with change in density?
- Is the amount of peak movement what you expect based on the density change?

b) Why do you think many-body correlations have the effect they do?

N1.4 Coordination numbers

These are defined as the integral of $g(r)$ in three dimensions over a specified radius range:-

$$N(R_1, R_2) = 4\pi\rho \int_{R_1}^{R_2} r^2 g(r) dr \quad (\text{N1.3})$$

The “running” coordination number at radius r is defined as $N(0, r)$, which is sometimes written simply as $N(r)$. Figure N1.2 shows the running coordination numbers for the RDFs of Figure N1.1

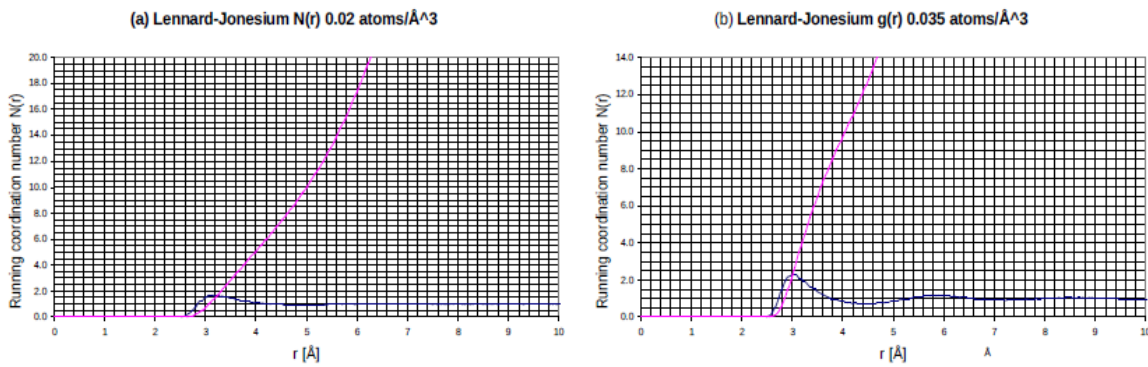


Figure N1.2

a) Using the grid provided estimate approximately the coordination number up to the first minimum in $g(r)$ for each of the cases shown in Figure N1.1 This is what is frequently quoted as the “coordination number” of the atom at each density. Do these numbers scale with the density?

b) If instead we had used the same distance range for both densities would the coordination numbers scale with density?

N1.5 The structure factor.

The diffraction experiment does not measure $g(r)$, but its Fourier transform, the structure factor, $H(Q)$, where

$$H(Q) = 4\pi\rho \int_0^{\infty} r^2 \left(g(r) - 1 \right) \frac{\sin Qr}{Qr} dr \quad (\text{N1.4})$$

where Q , the wavevector transfer in the diffraction experiment, is given by, $Q = 4\pi \sin \theta / \lambda$, with 2θ the detector scattering angle, and λ the radiation wavelength.

The structure factors corresponding to the two densities of Lennard-Jonesium in N1.3 are shown in Figure N1.3.

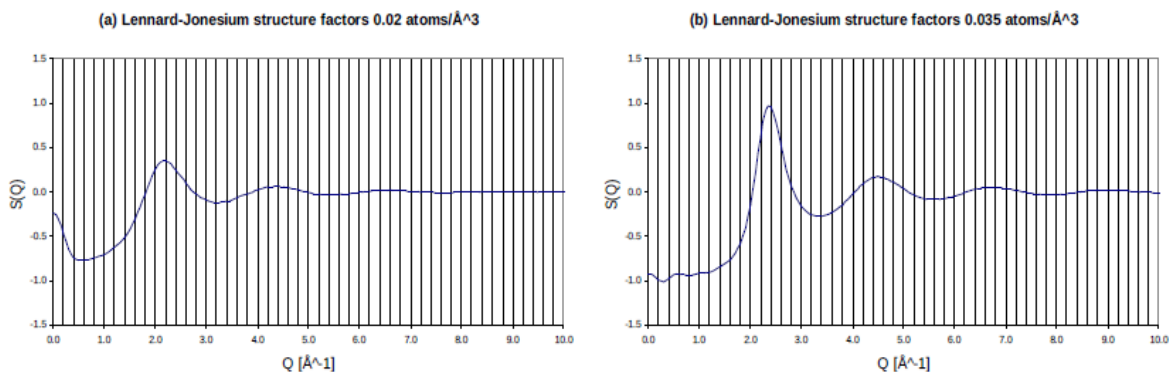


Figure N1.3

a) Describe the effect of changing the density on the structure factor. How does this compare with effect of changing the density on the radial distribution function?

b) What is the (approximate) relationship between the position of the first peak in $g(r)$ and the first (primary) peak in $H(Q)$?

c) What would happen to the position of the first peak in $H(Q)$ if we increased the value of σ ?

d) Given that the radial distribution function remains finite at all densities, using Eq. N1.4 what is the structure factor of an infinitely dilute gas?

N 2.

Two component systems: use of isotope substitution and the case of molten ZnCl_2 .

The diffraction pattern from a system containing 2 atomic components can be written as

$$F(Q) = c_1^2 \langle b_1 \rangle^2 H_{11}(Q) + 2c_1 c_2 \langle b_1 \rangle \langle b_2 \rangle H_{12}(Q) + c_2^2 \langle b_2 \rangle^2 H_{22}(Q) \quad (\text{N2.1})$$

where c_α is the atomic fraction and b_α is the neutron scattering length of component α , $H_{\alpha\beta}(Q)$ is the partial structure factor (psf), analogous to (1.4) above, for the pair of atoms α, β , defined by:

$$H_{\alpha\beta}(Q) = 4\pi\rho \int_0^\infty r^2 \left(g_{\alpha\beta}(r) - 1 \right) \frac{\sin Qr}{Qr} dr \quad (\text{N2.2})$$

and $g_{\alpha\beta}(r)$ is the site-site radial distribution function of β atoms about α . The brackets around the scattering lengths indicate that the scattering lengths have to be averaged over the spin and isotope states of each atomic component. The coordination number of β atoms about atom α can be defined in an analogous manner to Eq. N1.3

$$N_{\alpha\beta}(R_1, R_2) = 4\pi\rho c_\beta \int_{R_1}^{R_2} r^2 g_{\alpha\beta}(r) dr \quad (\text{N2.3})$$

A general rule is that if there are N distinct atomic components in a system, then there are $N(N+1)/2$ site-site radial distribution functions and partial structure factors to be determined. By “distinct atomic components” we do not necessarily mean atom types. For example a methyl hydrogen atom on an alcohol molecule is distinct from the point of view of the structure to a hydroxyl hydrogen atom, even though they are the same atom type.

N2.1 A classic example of the application of the isotope substitution method to a two-component liquid is the molten ZnCl_2 experiment of Biggin and Enderby (J. Phys. C: Solid State Phys., 14, 3129-3136 (1981)).

a) What are the atomic fractions of Zn and Cl in ZnCl_2 salt?

b) Hence, based on Eq. N2.1, write down a formula for the diffraction pattern of ZnCl_2 in terms of the Zn-Zn, Zn-Cl and Cl-Cl partial structure factors.

c) Given that two isotopes of chlorine are available, ^{35}Cl and ^{37}Cl , with markedly different scattering lengths (11.65fm and 3.08fm respectively) briefly explain how you might extract the three partial structure factors for ZnCl_2 experimentally.

d) Are there any other experimental techniques that could be used to do this?

N2.2 Figure N2.1 shows the actual diffraction data of Biggin and Enderby, while Table N1 below lists the neutron weights outside each partial structure factor for each of the Biggin and Enderby samples:

Table N1

Sample	At% ^{35}Cl [%]	At% ^{37}Cl [%]	Individual psf weighting factors [barns/sr/atom] [†]		
			Zn-Zn	Zn-Cl	Cl-Cl
Zn $^{35}\text{Cl}_2$	99.3	0.7	0.0358	0.2929	0.5982
ZnMixCl $_2$	67.7	32.3	0.0358	0.2253	0.3541
Zn $^{37}\text{Cl}_2$	2.7	97.3	0.0358	0.0837	0.0489

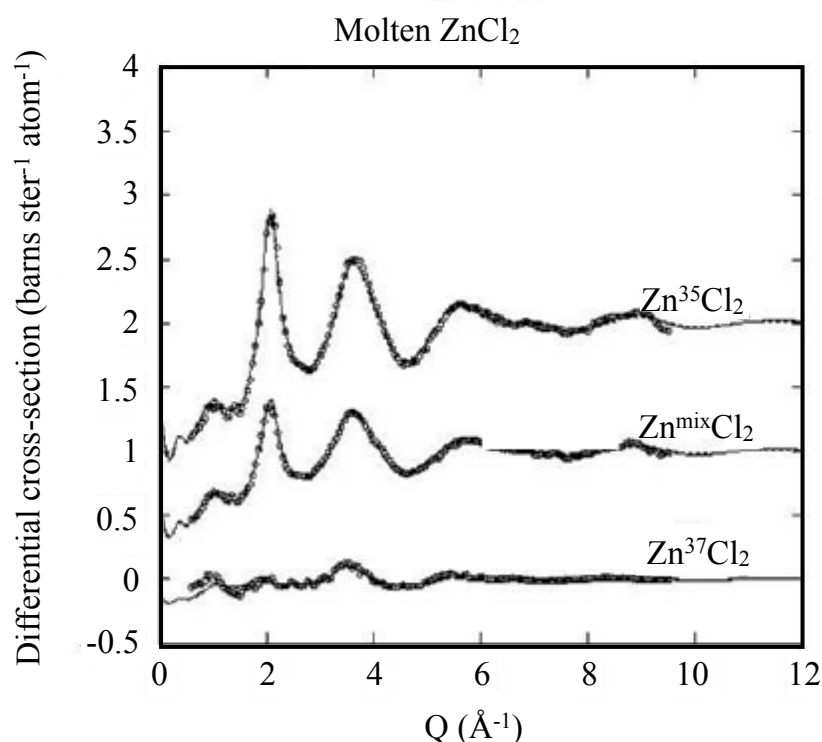


Figure N2.1 Diffraction data (points) for molten zinc chloride using different mixtures of chlorine isotopes. The line is a modern fit to these data using an EPSR (empirical potential structure refinement) computer simulation.

a) On the basis of the numbers in this table describe any problems that might arise in attempting to invert the diffraction data to partial structure factors. Look also at the diffraction data themselves, in Figure N2.1.

b) Given those reservations, what might happen when we try to convert the extracted partial structure factors to radial distribution functions using the inverse Fourier transform:

$$g_{\alpha\beta}(r) = 1 + \frac{1}{2\pi^2\rho} \int_0^\infty Q^2 H_{\alpha\beta}(Q) \frac{\sin Qr}{Qr} dQ \quad (\text{N2.4})$$

c) Describe another method that might be used to separate out the site-site radial distribution functions from the measured diffraction data.

N2.3 Figure N2.2 shows a computer simulation of the radial distribution functions and running coordination numbers of molten zinc chloride, ZnCl_2 , as derived from the Biggin and Enderby diffraction data.

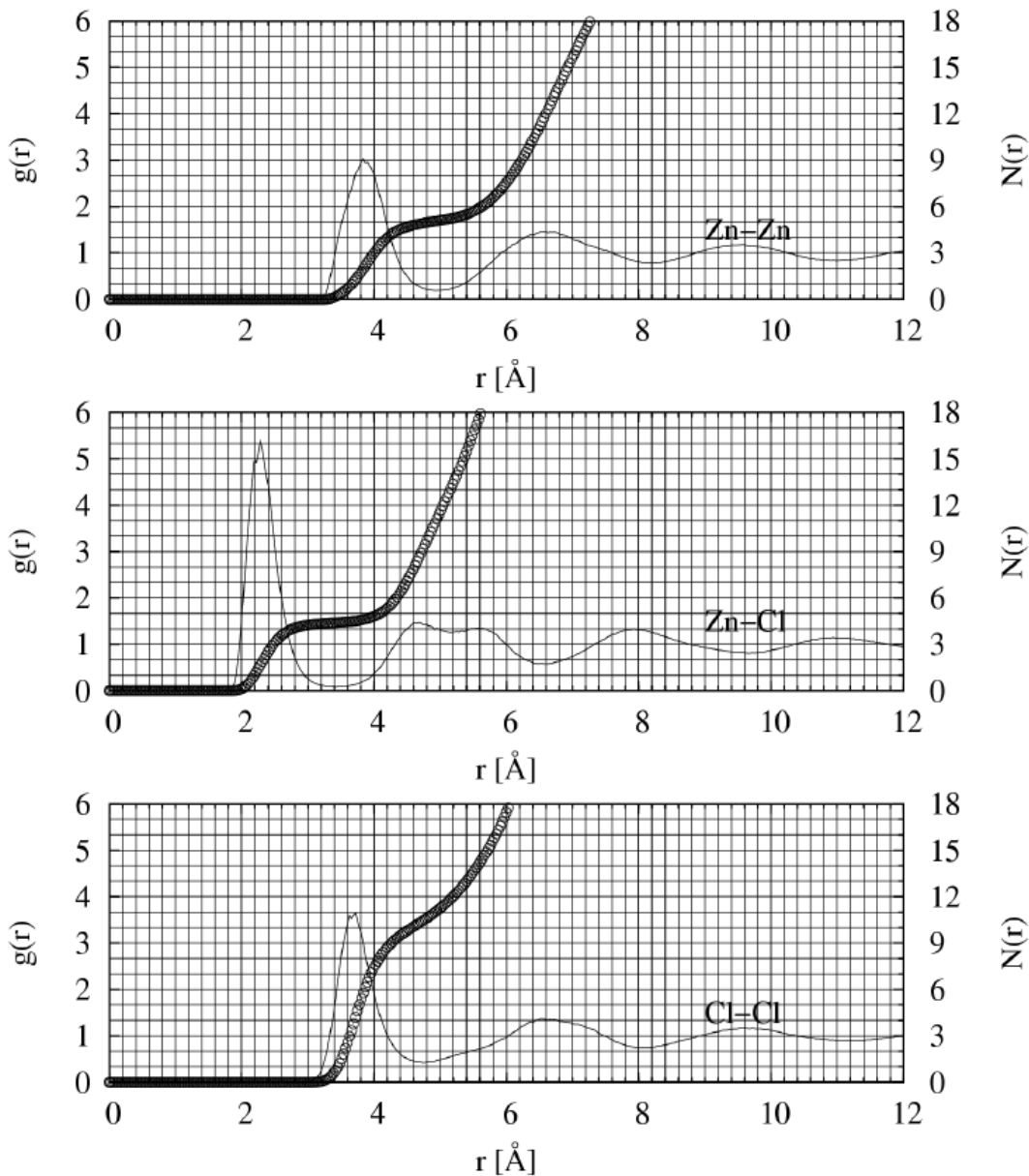


Figure N2.2 Radial distribution functions (lines, left-hand scale) and running coordination numbers (point, right-hand scale) for molten zinc chloride.

- a) Using the grid, or other method, estimate approximately the coordination number of Cl around Zn. What would be the corresponding coordination number of Zn around Cl?
- b) Given this number, and the position of the Zn-Zn and Cl-Cl first peaks, what can you say about the local structure in molten ZnCl_2 ?
- c) For the region beyond the first peaks, what do you notice about the three site-site rdfs for molten ZnCl_2 ? Use this to speculate on what might be happening to the ordering of the Zn and Cl atoms.